SURPRISES: When *ab-initio* meets statistics in extended systems

Quantum Monte Carlo in the Apuan Alps VI
30/07/2010, TTI

Simone Taioli
taioli@fbk.eu

http://ctp.fbk.eu

Interdisciplinary Laboratory for Computational Science (LISC)
FBK-CMM and University of Trento
now @ UCL at Dario's

OUTLINE

- Bird's eye view on core-electron spectroscopies.
- A new theoretical method for calculating electron spectra in solids: QMMC.
- Guided by my own experience I have chosen two applications:
  - Auger spectra of SiO_2 nanoclusters: chemical recognition.
  - Growth and electronic properties of carbon-based materials.

Spectroscopies

- Tools for investigating properties of matter by the interaction with projectiles.
- Which matter? XPS, Auger and EELS spectra can be recorded on atoms, molecules and solid samples.
- Which projectiles? Impinging particles may be photons, electrons, neutrons, ions.....

Spectroscopies

- The totality of physical and chemical processes involve the scattering or the transfer of "particles".
- Scattering of particles and dynamics are connected:
  - the former is a very powerful tool for investigating and originating the latter.
  - The energy and time domain are linked by a FT.
  - The e/de-xcitation are inherently many-body phenomena.
- Chemical elements recognition:
  - Information on the electronic structure of materials.
  - Quantitative determination of the impurities in a sample.

Spectroscopies

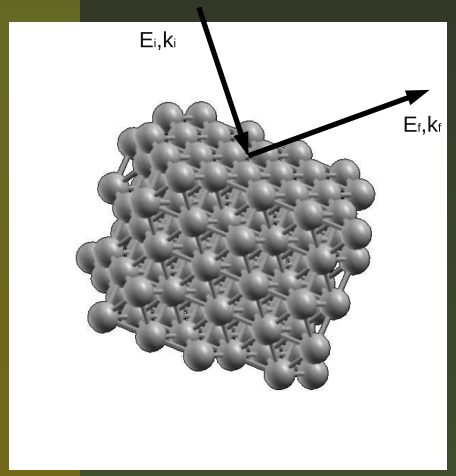

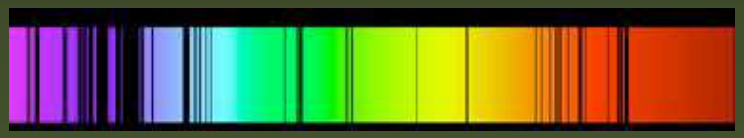

- Elastic scattering: $E_i = E_f$ and $q_i = q_f$, E_i continuous
- Inelastic scattering: $E_i \neq E_f$ and $q_i \neq q_f$, E_f discrete
- Mechanisms: ionization, electron excitations, plasmons, ...

Basics for e^- spectroscopy

- A device for producing the electronic or photonic beam, at typical energies between 1 and 30 keV necessary for the primary ionization; the same energy range is needed in EELS to travel well inside the material.
- A target constituted by a solid sample or by a supersonic beam of atoms or molecules;
- A spectrometer or analyzer, that collects the electrons emitted by the target after the collision.

Microscopic Observables

- the differential cross section is defined by the probability to observe a scattered particle into a solid angle unit if the target is irradiated by a flux of one particle by surface unit

$$\frac{d\sigma}{d\Omega} = \frac{Scattered\ flux/Unit\ solid\ angle}{Incident\ flux/Unit\ of\ surface}$$

- the double differential cross section $\frac{d^2\sigma}{d\Omega dE}$ is the differential cross section within a unit energy range

Microscopic Observables

- the differential cross section is defined by the probability to observe a scattered particle into a solid angle unit if the target is irradiated by a flux of one particle by surface unit

$$\frac{d\sigma}{d\Omega} = \frac{Scattered\ flux/Unit\ solid\ angle}{Incident\ flux/Unit\ of\ surface}$$

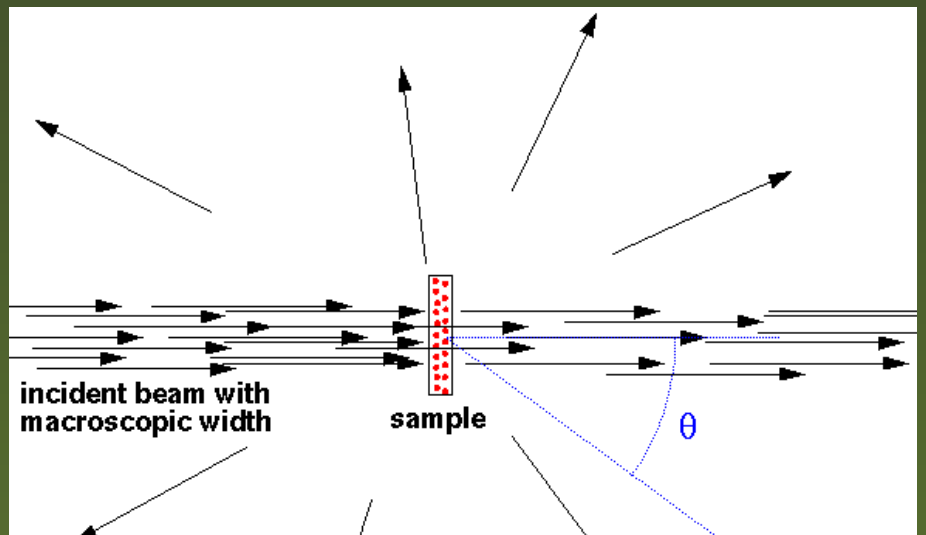

Macroscopic Observables

Absorption: $I = I_0 \exp(-\alpha x)$ where α depends on the sample (imaginary part of the dielectric constant ϵ)

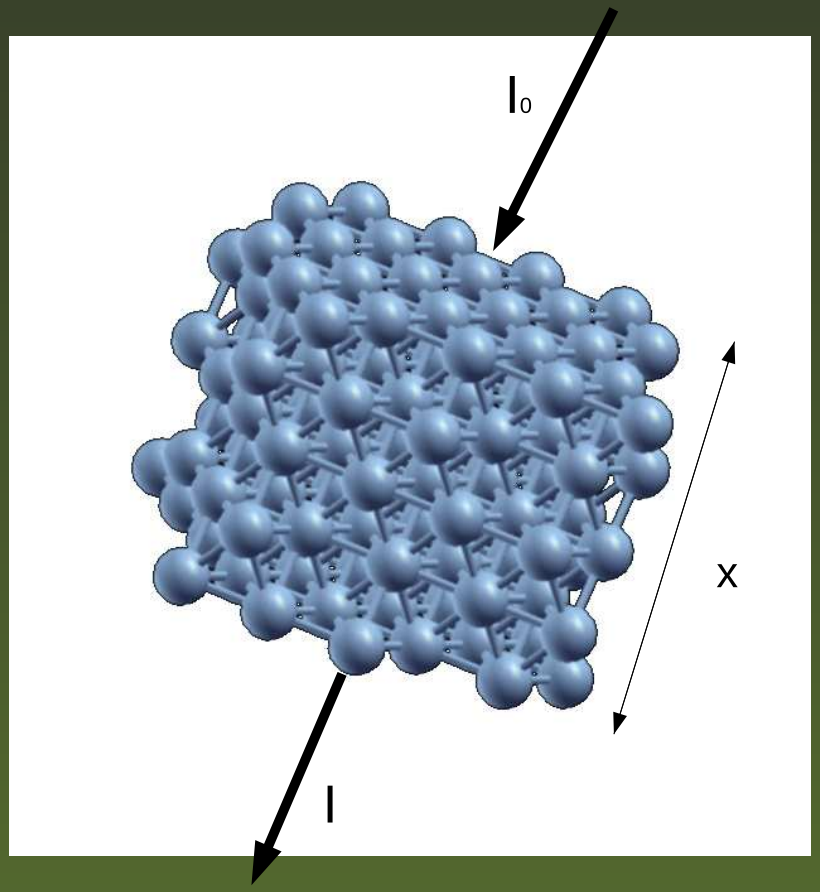

Micro-Macro Connection

- Connection between the micro-world in linear response (band structures and wavefunctions), and the macroscopic optical constants (absorption coefficient (ABS) and energy loss (ELF)) is:

$$\begin{aligned} ELF &= -\mathrm{Im}\left(\frac{1}{\epsilon_{av}}\right) \\ ABS &= \mathrm{Im}\left(\epsilon_{av}\right). \end{aligned}$$

- α is related to the macroscopic frequency-dependent dielectric function ϵ_{av}
- ϵ_{av} gives a connection between macroscopic theory, based on Maxwell's equations, and the long wavelength limit of the microscopic dielectric function ($\mathbf{G}' = \mathbf{q} + \mathbf{G}$):

$$\epsilon_{\mathbf{G},\mathbf{G}'}(\mathbf{q},\omega) = \frac{8\pi^2}{\Omega}\frac{1}{q^2}\sum_{v,c,\mathbf{G}} |<c,\mathbf{G}+\mathbf{q}|\exp^{i\mathbf{q}\cdot\mathbf{r}}|v,\mathbf{G}>|^2 \delta(\epsilon_{c,\mathbf{G}+\mathbf{q}} - \epsilon_{v,\mathbf{G}} - \omega)$$

Processes by photon impact

- $h\nu \; + \; AB \longrightarrow e^{-}_{core} \; + \; AB^{+*}$ (A)
- $h\nu \; + \; AB \longrightarrow AB^{*}$ (B)
- $AB^{+*} \longrightarrow e^{-}_{Auger} \; + \; AB^{++*}$ (A$'$)
- $AB^{*} \longrightarrow e^{-} \; + \; AB^{+*}$ (B$'$)

Processes by photon impact

- $h\nu + AB \longrightarrow e^-_{core} + AB^{+*}$ (A)
- $h\nu + AB \longrightarrow AB^*$ (B)
- $AB^{+*} \longrightarrow e^-_{Auger} + AB^{++*}$ (A$'$)
- $AB^* \longrightarrow e^- + AB^{+*}$ (B$'$)

(A) PRIMARY PHOTOEMISSION

Processes by photon impact

- $h\nu + AB \longrightarrow e^-_{core} + AB^{+*}$ (A)
- $h\nu + AB \longrightarrow AB^*$ (B)
- $AB^{+*} \longrightarrow e^-_{Auger} + AB^{++*}$ (A$'$)
- $AB^* \longrightarrow e^- + AB^{+*}$ (B$'$)

(B) PRIMARY PHOTO-EXCITATION

Processes by photon impact

- $h\nu + AB \longrightarrow e^-_{core} + AB^{+*}$ (A)
- $h\nu + AB \longrightarrow AB^*$ (B)
- $AB^{+*} \longrightarrow e^-_{Auger} + AB^{++*}$ (A$'$)
- $AB^* \longrightarrow e^- + AB^{+*}$ (B$'$)

(C) NORMAL AUGER EMISSION

Processes by photon impact

- $h\nu + AB \longrightarrow e^-_{core} + AB^{+*}$ (A)
- $h\nu + AB \longrightarrow AB^*$ (B)
- $AB^{+*} \longrightarrow e^-_{Auger} + AB^{++*}$ (A$'$)
- $AB^* \longrightarrow e^- + AB^{+*}$ (B$'$)

(D) AUTOIONIZATION

Photon-matter interactions

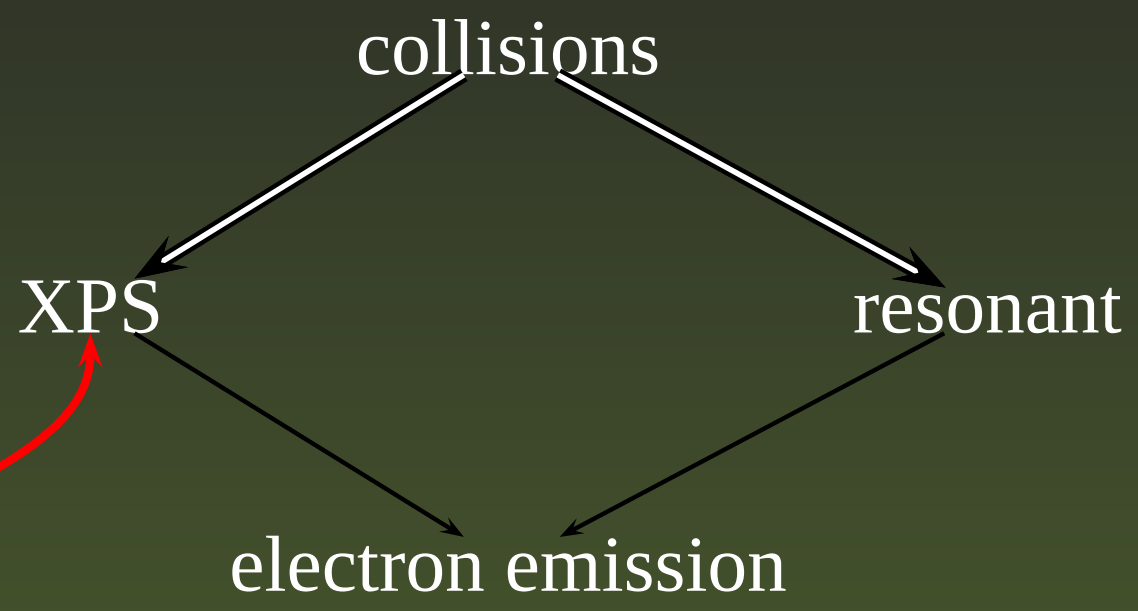

Direct processes: the spectrum is a fingerprint of the material $\Longrightarrow$ can be used to investigate chemical bonds, adsorption via core-level shifts...

Photon-matter interactions

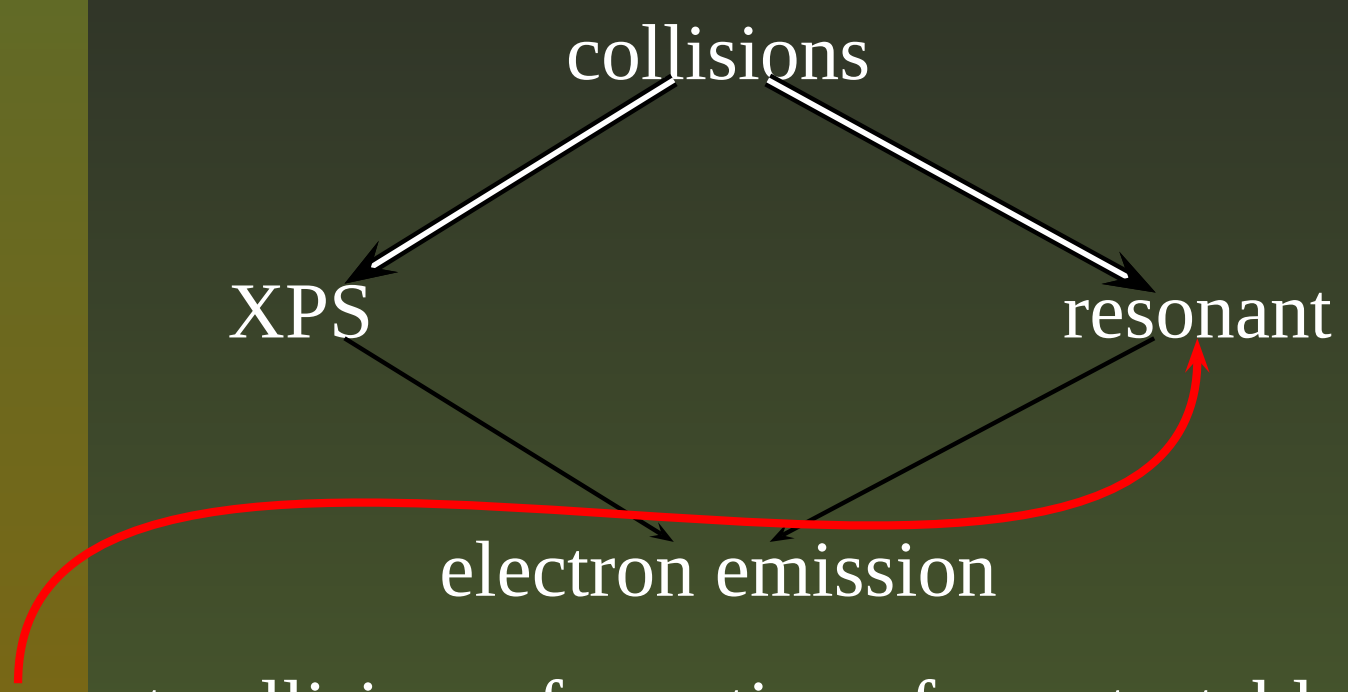

Resonant collisions: formation of a metastable system embedded in the continuum of higher charge state $\Longrightarrow$ can be used to investigate electron dynamics, many-body effects, chemical environment...

Photon-matter interactions

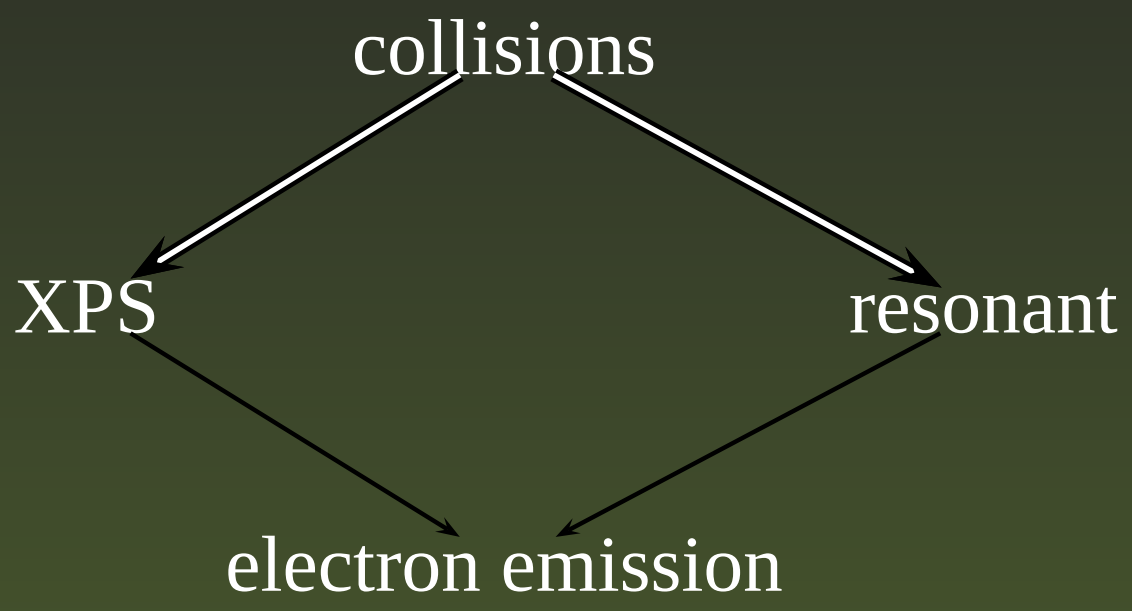

- Electron decay times can commensurate with molecular vibrational period: importance of nuclear dynamics in polyatomic systems.

Photon-matter interactions

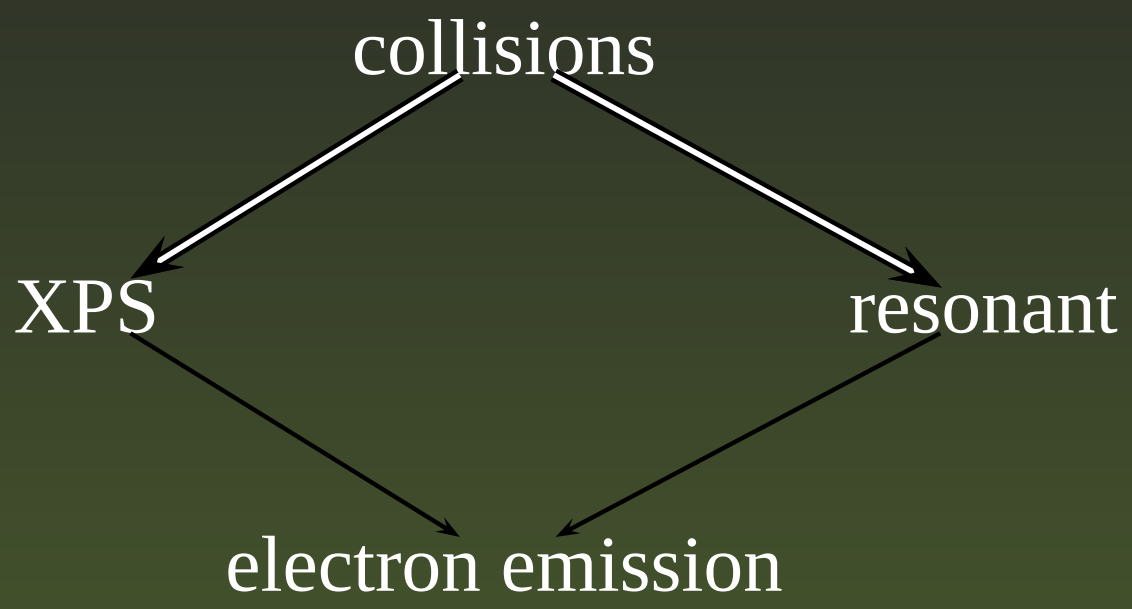

The escaping electrons may suffer further inelastic collisions with surrounding electronic cloud and collective charge motion.

Photon-matter interactions

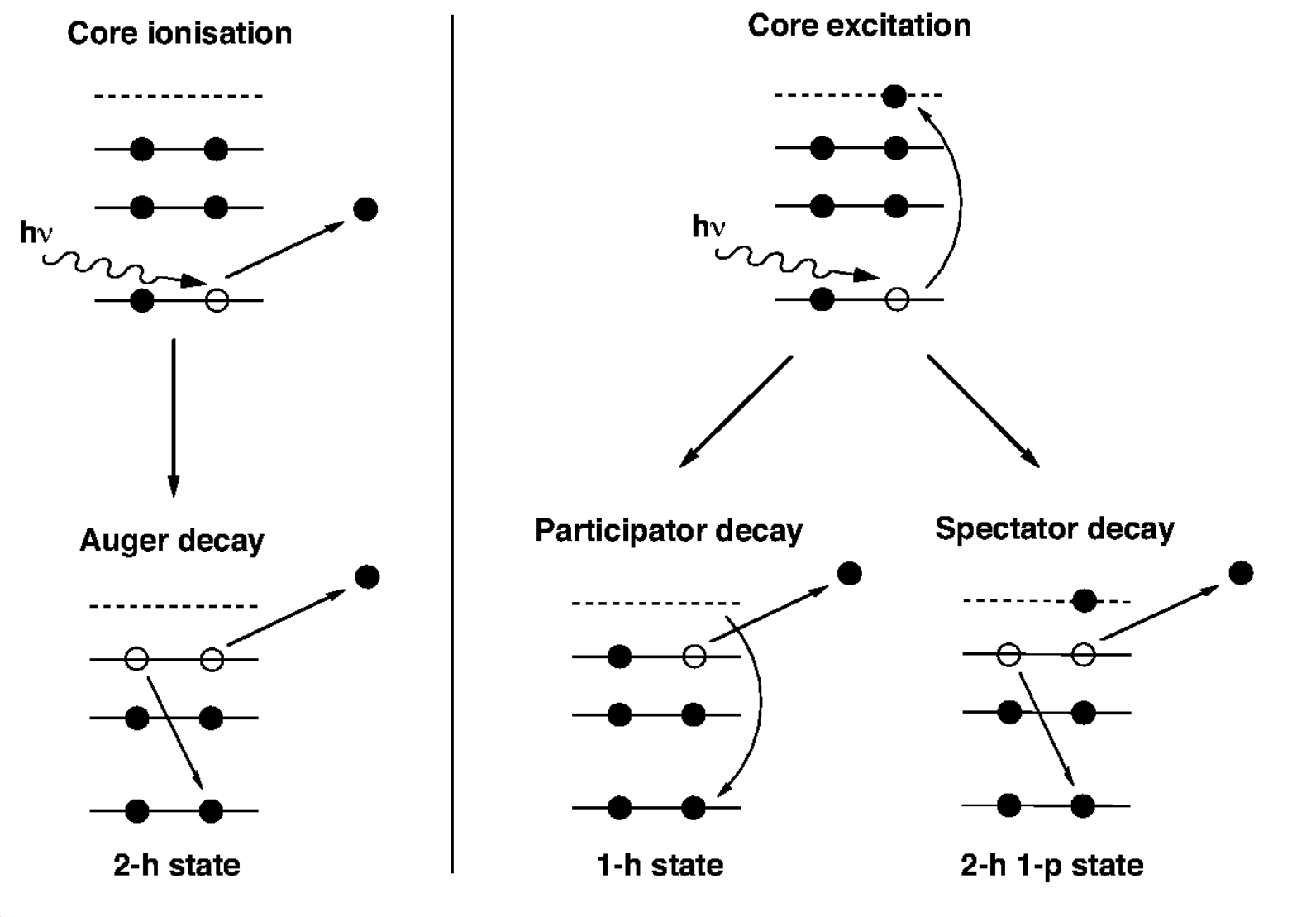

CO XPS-C K shell spectra

$$BE = h\nu - E_{kin},\ \Gamma = 0.054\,eV,\ \gamma_0 = 0.35\,eV$$

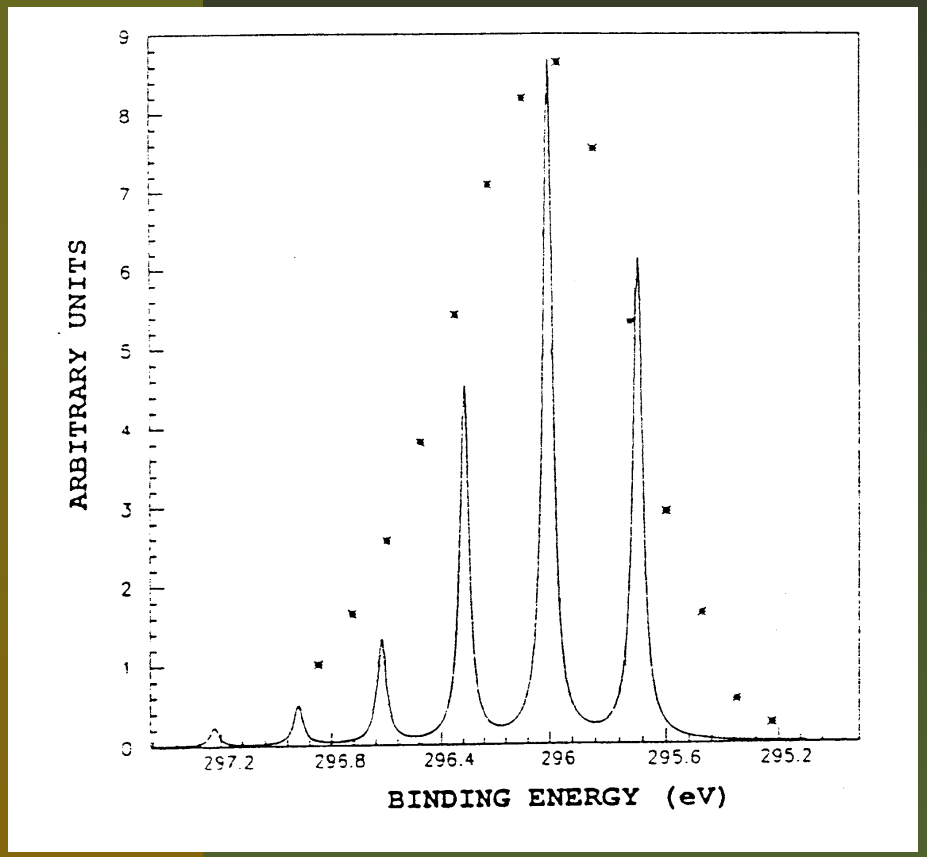

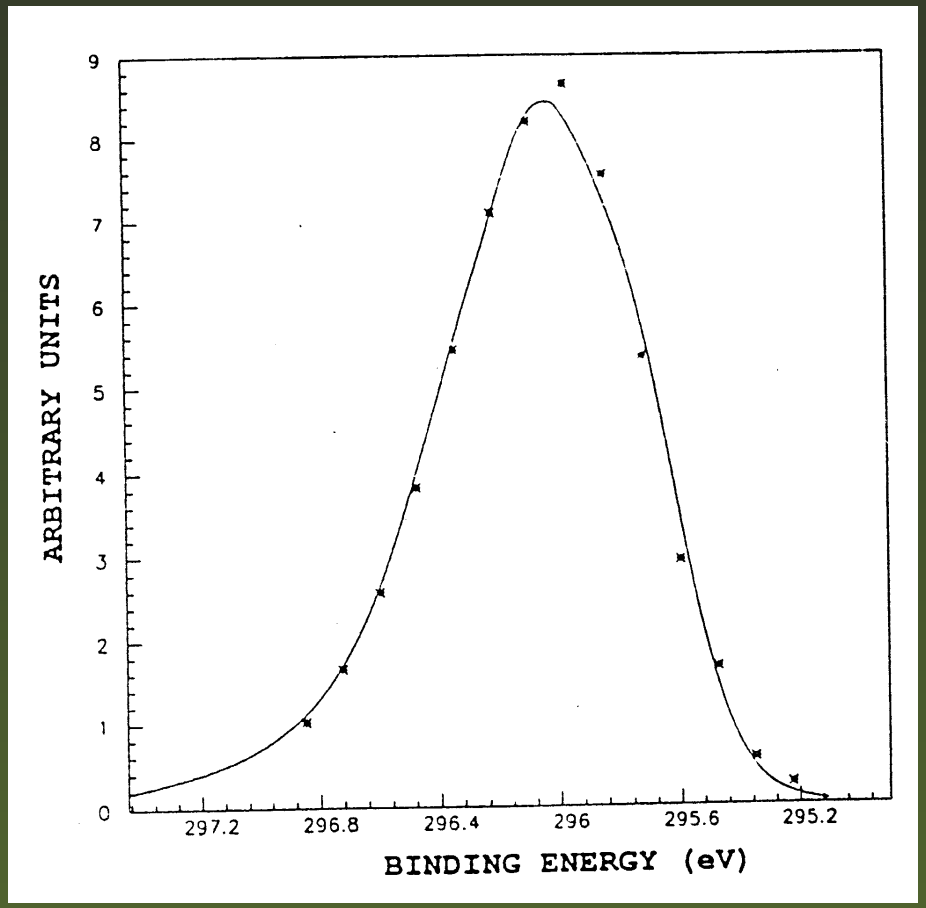

CO XPS-O K shell spectra

$$BE = h\nu - E_{kin},\ \Gamma = 0.065\ eV,\ \gamma_0 = 0.35\ eV$$

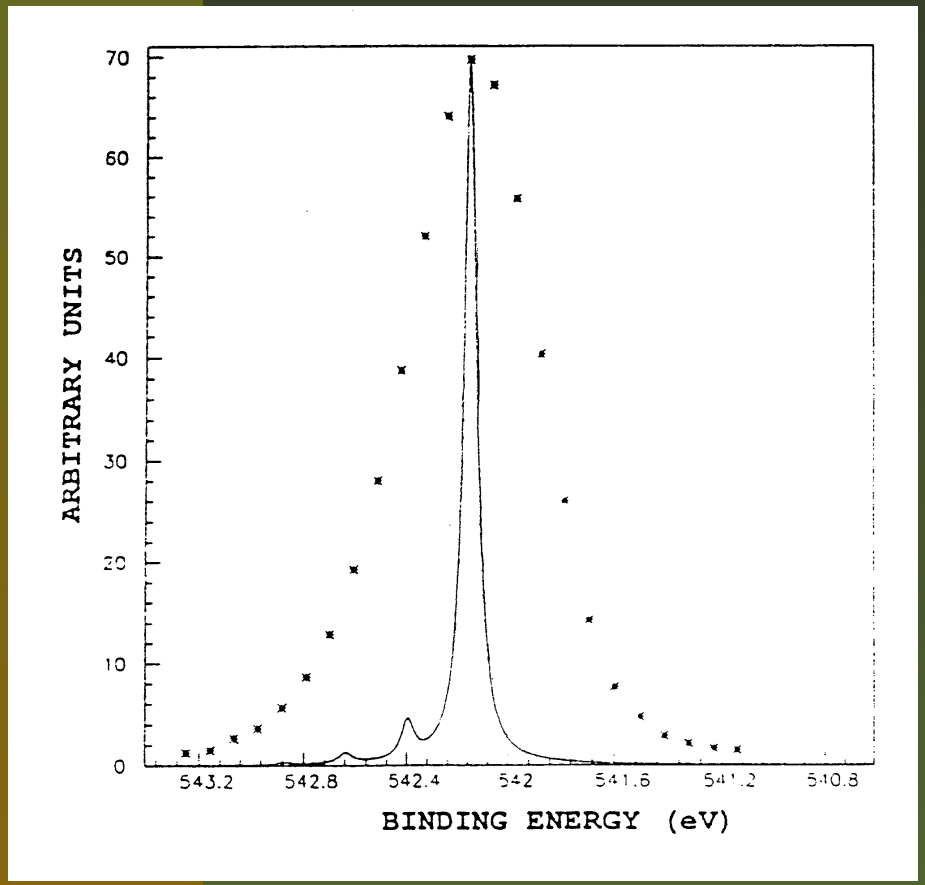

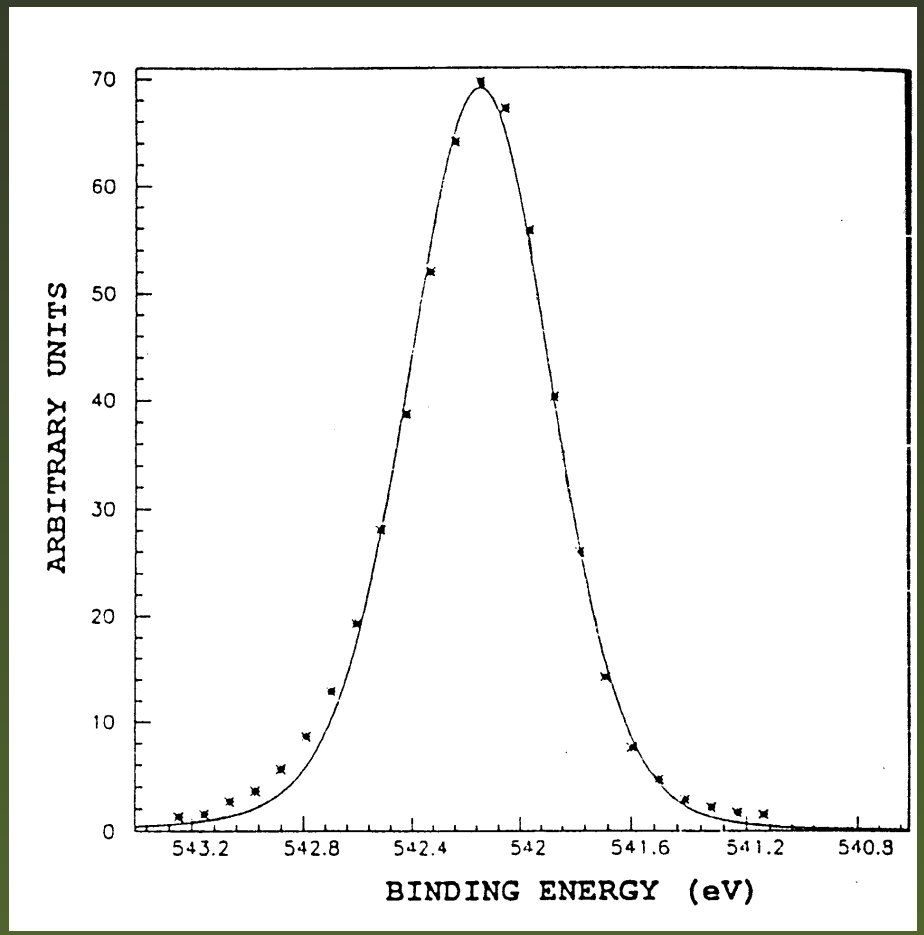

CO Auger C K-LL spectra

$$E_{Auger} = E_L + E_{L'} - E_K$$

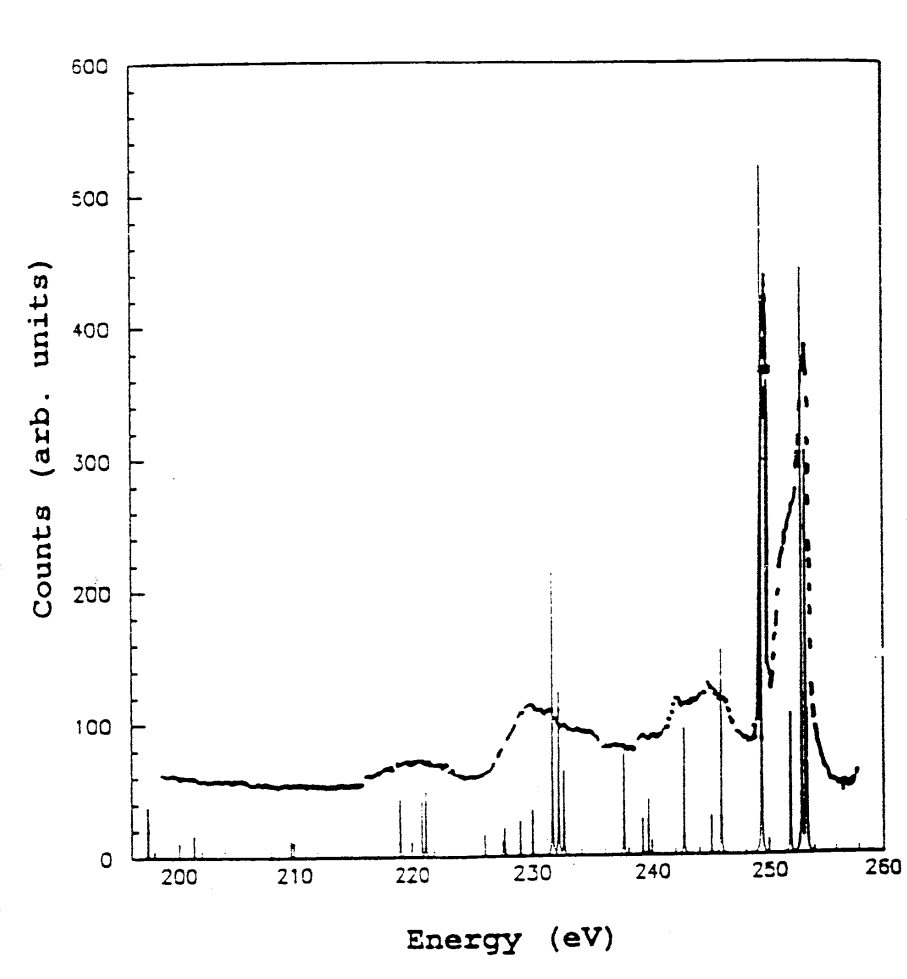

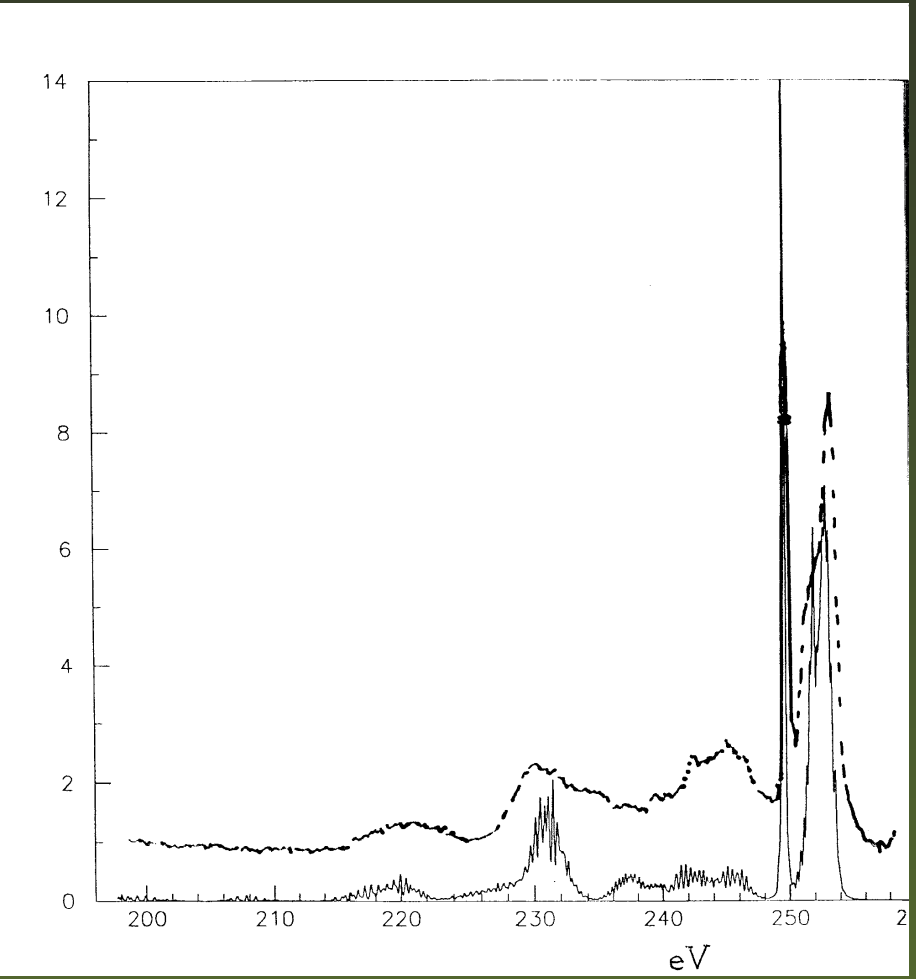

CO Auger O K-LL spectra

$$E_{Auger} = E_L + E_{L'} - E_K$$

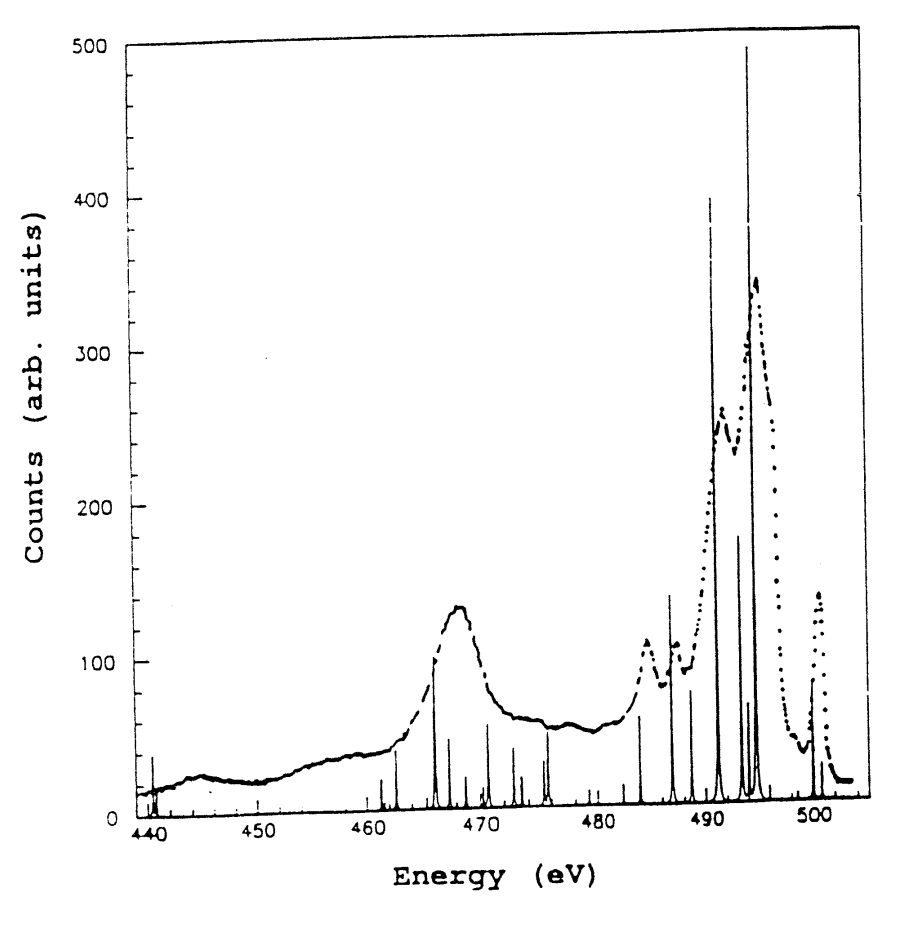

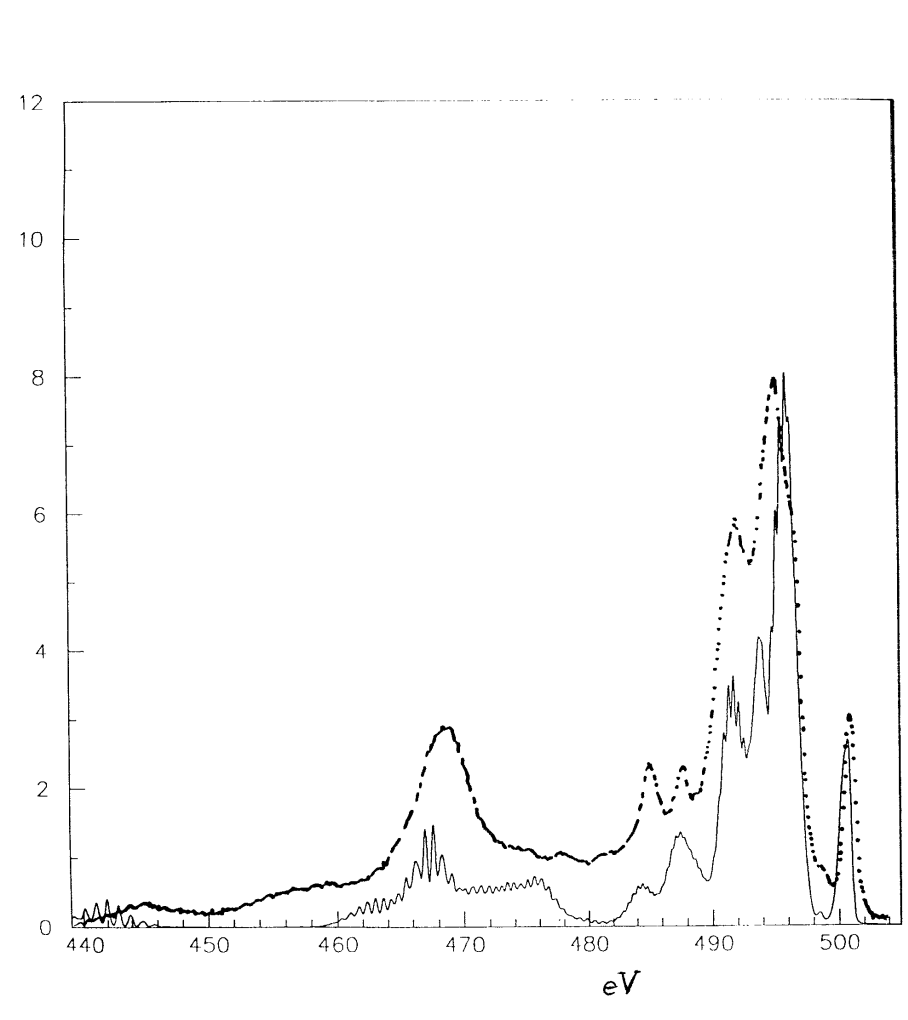

Atomic Oxygen XPS K-shell spectra

BE is a function of the chemical environment of atoms

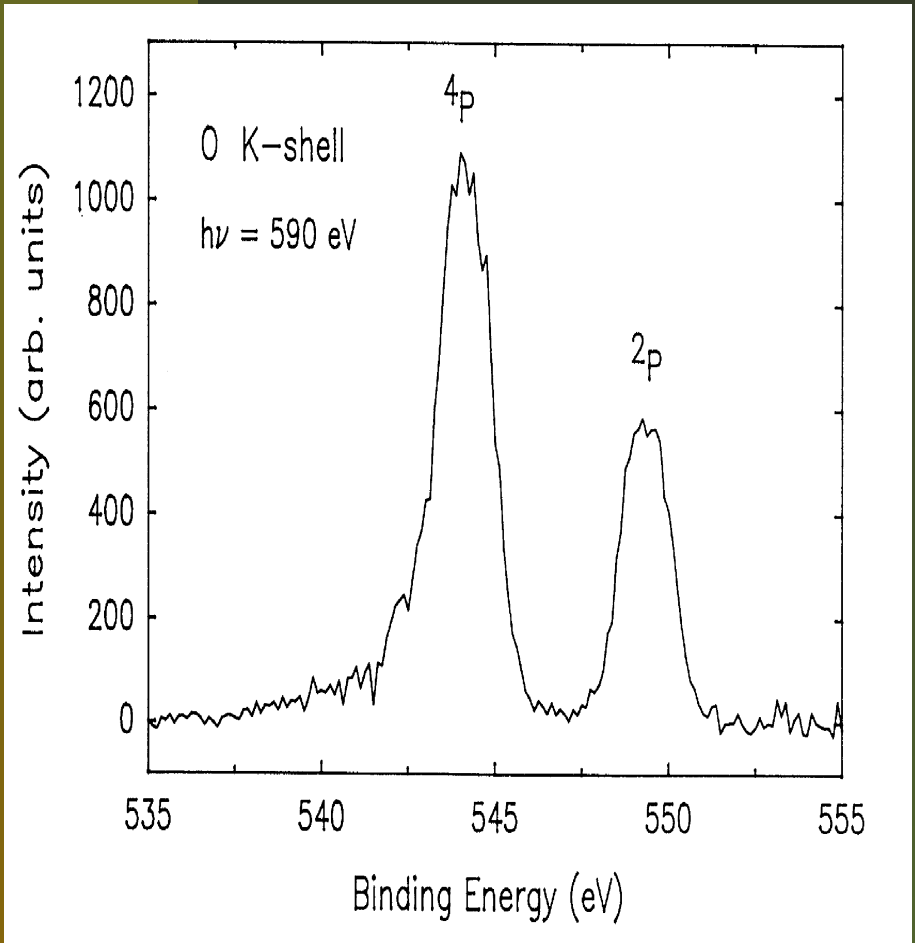

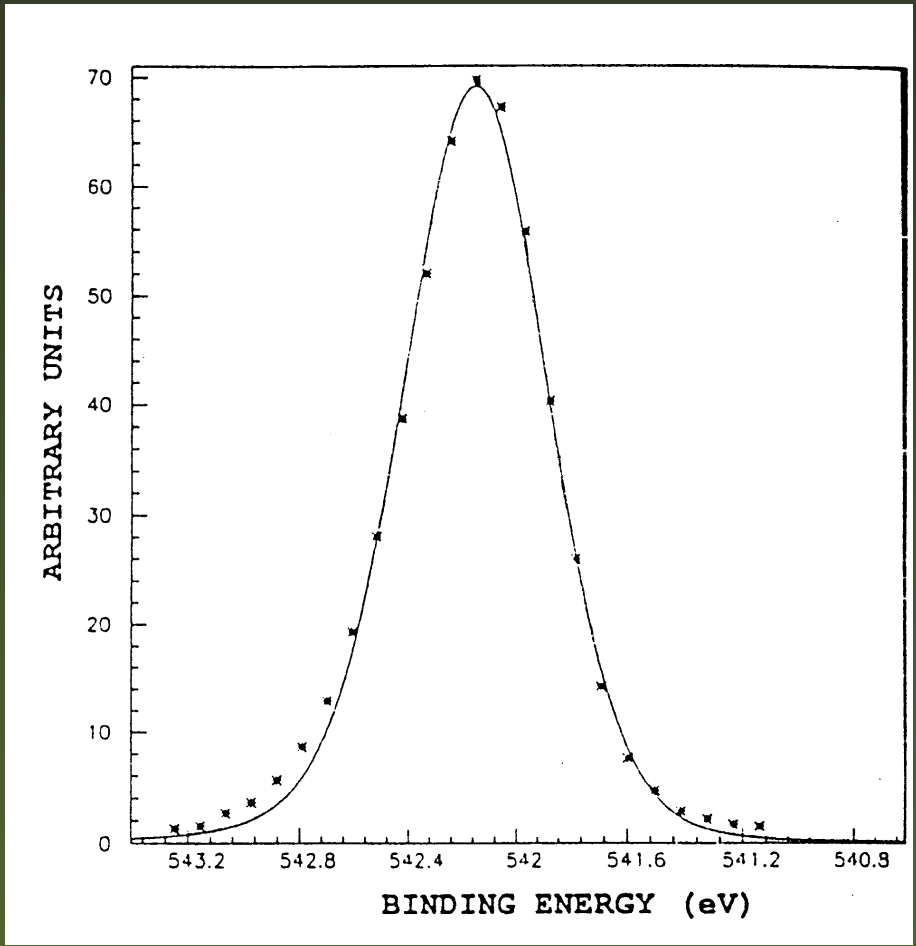

Atomic O Auger K-LL spectra

Auger E_{kin} is a function of the chemical environment of atoms

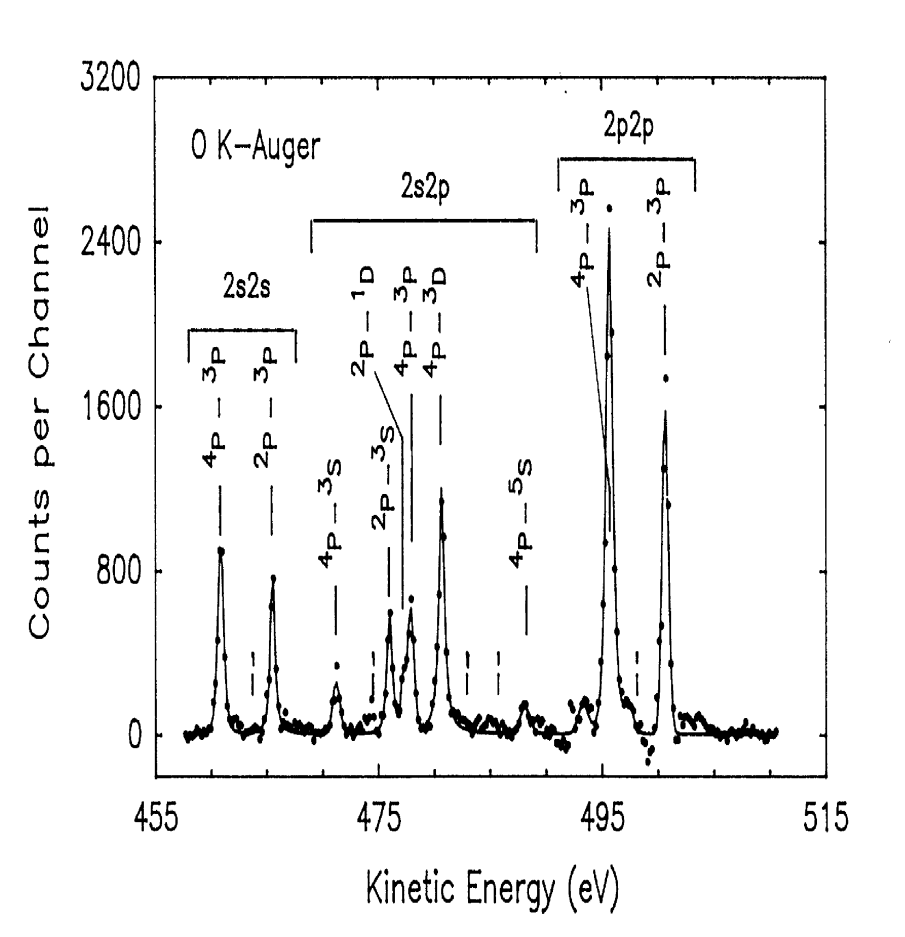

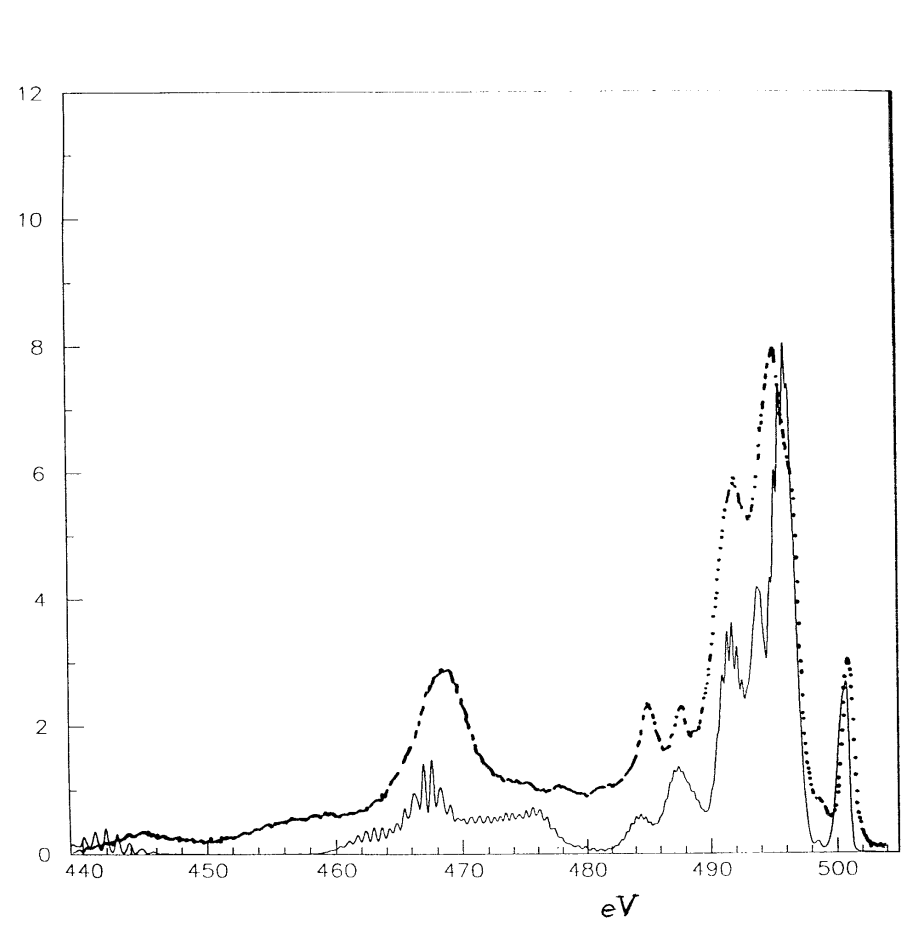

EELS

- EEL spectroscopy is of primary importance in the characterization of materials.
- It is characterized by many features: multiple scattering, single electron excitations and anisotropy effects.
- Inelastic and elastic processes can be identified via the energy loss function.
- The most relevant is the plasmon peak energy.
- $\varepsilon(\mathbf{k}, \omega)$, dielectric function = response of conduction electrons to the electric field (ω = frequency) due to electrons ($\mathbf{k}$ = wave vector) passing through a solid and losing energy in it.

EELS

- The e^- passing through can be represented by:

$$\rho(\mathbf{r}, t) \;=\; -e\,\delta(\mathbf{r} - \mathbf{v}t)$$

  $\mathbf{r}$ and $\mathbf{v}$ = position and speed of e^- at time t.

- The electric potential generated in the medium is

$$\varepsilon(\mathbf{k}, \omega)\,\nabla^2\varphi(\mathbf{r}, t) \;=\; -4\pi\,\rho(\mathbf{r}, t) \;=\; 4\pi\,e\,\delta(\mathbf{r} - \mathbf{v}t)\,.$$

- The EEL per unit path length dx for the interaction with $\mathbf{E}$ generated by the electrons passing through the solid is given by

$$-\frac{dW}{dx} \;=\; \frac{e}{v}\,\mathbf{v}\,\cdot\,\mathbf{E}\,.$$

EELS

- From the Poisson equation in the Fourier space:

$$-\frac{dW}{dx} = \frac{e^2}{\pi^2 v} \int d\mathbf{k} \int_0^\infty d\omega\, \omega\, \mathrm{Im}\left[\frac{1}{\varepsilon(\mathbf{k},\omega)}\right] \frac{\delta(\mathbf{k}\cdot\mathbf{v}+\omega)}{k^2}$$

- The electron inverse inelastic mean free path is:

$$\lambda_{inel}^{-1} = \frac{m\, e^2}{\pi\, \hbar^2\, T} \int_0^{W_{max}} dW \int_{\hbar\, k_-}^{\hbar\, k_+} \frac{dk}{k}\, \mathrm{Im}\left[\frac{1}{\varepsilon(k,\omega)}\right]$$

and the differential inelastic scattering cross section

$$\frac{d\sigma_{inel}}{dW} = \frac{1}{N\, \pi\, T\, a_0} \int_{k_-}^{k_+} \frac{dk}{k}\, \mathrm{Im}\left[\frac{1}{\varepsilon(k,\omega)}\right]$$

N = target density, a_0 = Bohr radius.

Dielectric function (Drude model)

- The electric displacement $\mathbf{D}$ is

$$\mathbf{D} = \mathbf{E} + 4\pi\mathbf{P} = (1 + 4\pi\chi)\,\mathbf{E} = \varepsilon\,\mathbf{E}$$

  where the polarization density of the material is $P = e\,n\,\xi$, where n = electron density, ξ = electron displacement

- For elastically bound electrons

$$m\,\ddot{\xi} + \beta\dot{\xi} + k\,\xi = e\,E(t)$$

  where $\beta = m\,\gamma$, $k_n = m\,\omega_n^2$ = elastic constant, m = electron mass, ω_n = natural frequencies and γ = damping constant due to collisions, irradiation....

Dielectric function

- Finally, for finite electron moment

$$\varepsilon(k,\omega) \;=\; 1 \;-\; \omega_p^2 \sum_n \frac{f_n}{\omega^2 \;-\; \omega_n^2 \;-\; \omega_k^2 \;-\; i\gamma_n\omega}\,.$$

where $\omega_p = \sqrt{\frac{4\,\pi\,n\,e^2}{m}}$ is the plasma frequency

- One can try an ab-initio calculation for the energy-dependent dielectric function.

Secondary Electrons Spectroscopies

LEED=Low Energy Electron Diffraction (elastic scattering $E = E_0$)

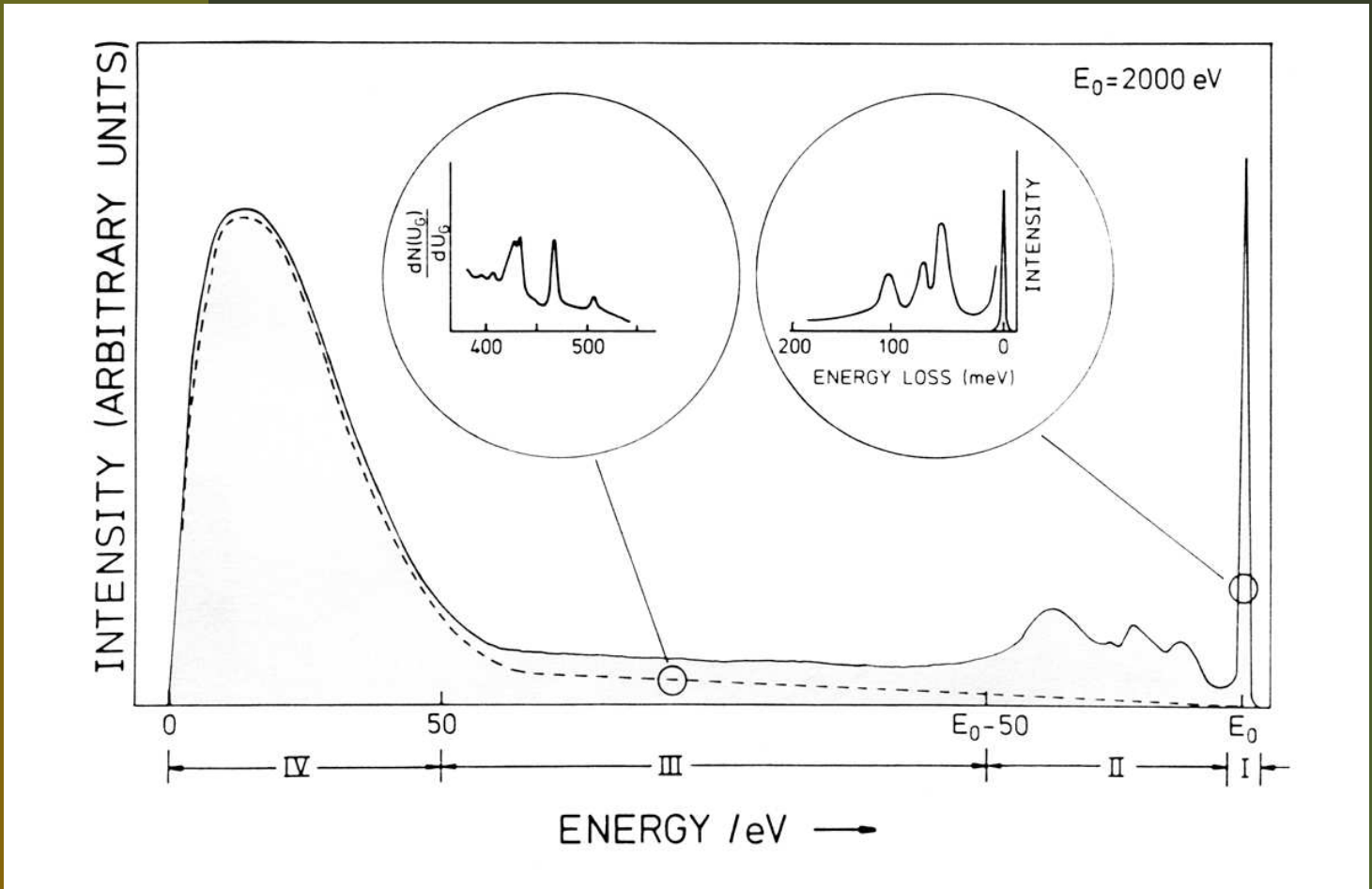

Secondary Electrons Spectroscopies

EELS=Electron Energy Loss Spectroscopy (inelastic scattering due to plasmons $E_0 - 50\ eV \leq E \leq E_0$)

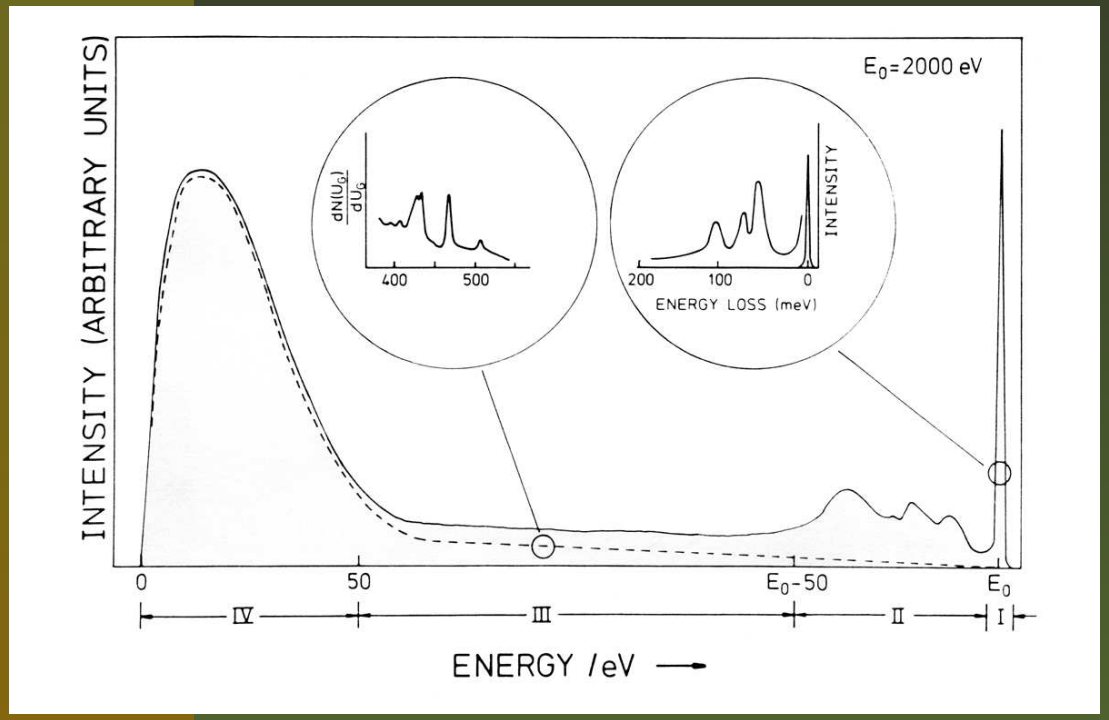

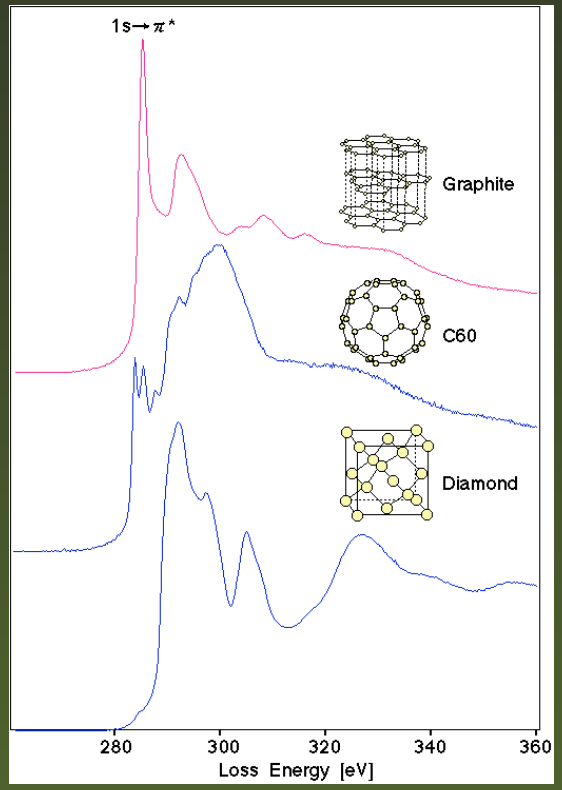

Secondary Electrons Spectroscopies

HREELS=High Resolution Electron Energy Loss Spectroscopy (inelastic scattering due to phonons $E_0 - 0.1\,eV \leq E \leq E_0$)

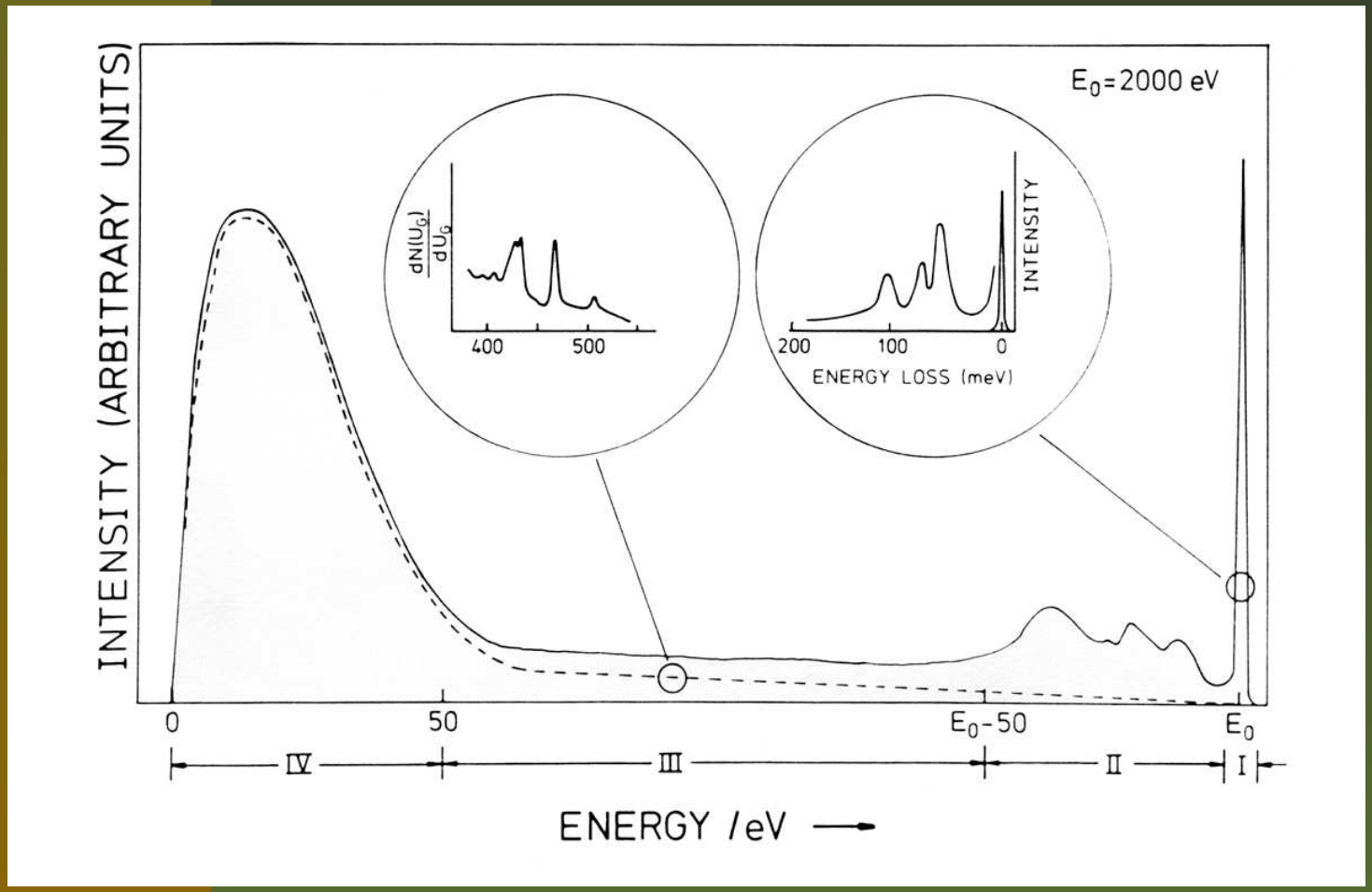

Secondary Electrons Spectroscopies

AES=Auger Electron Spectroscopy
($50\ eV \leq E \leq E_0 - 50\ eV$)

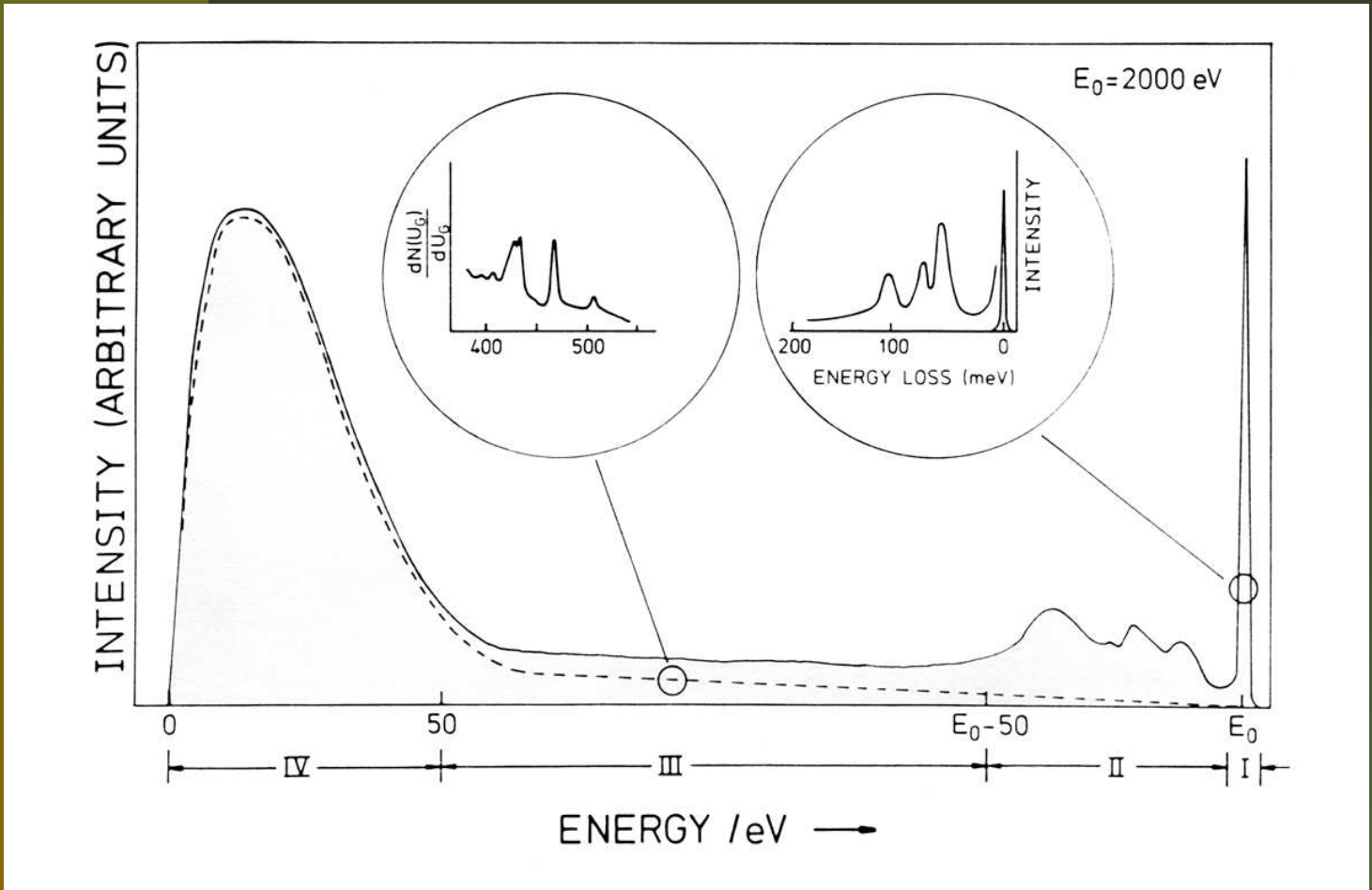

Secondary Electrons Spectroscopies

SEM=Scanning Electron Microscopy (true secondary electrons originating from cascade processes $0 \leq E \leq 50\ eV$)

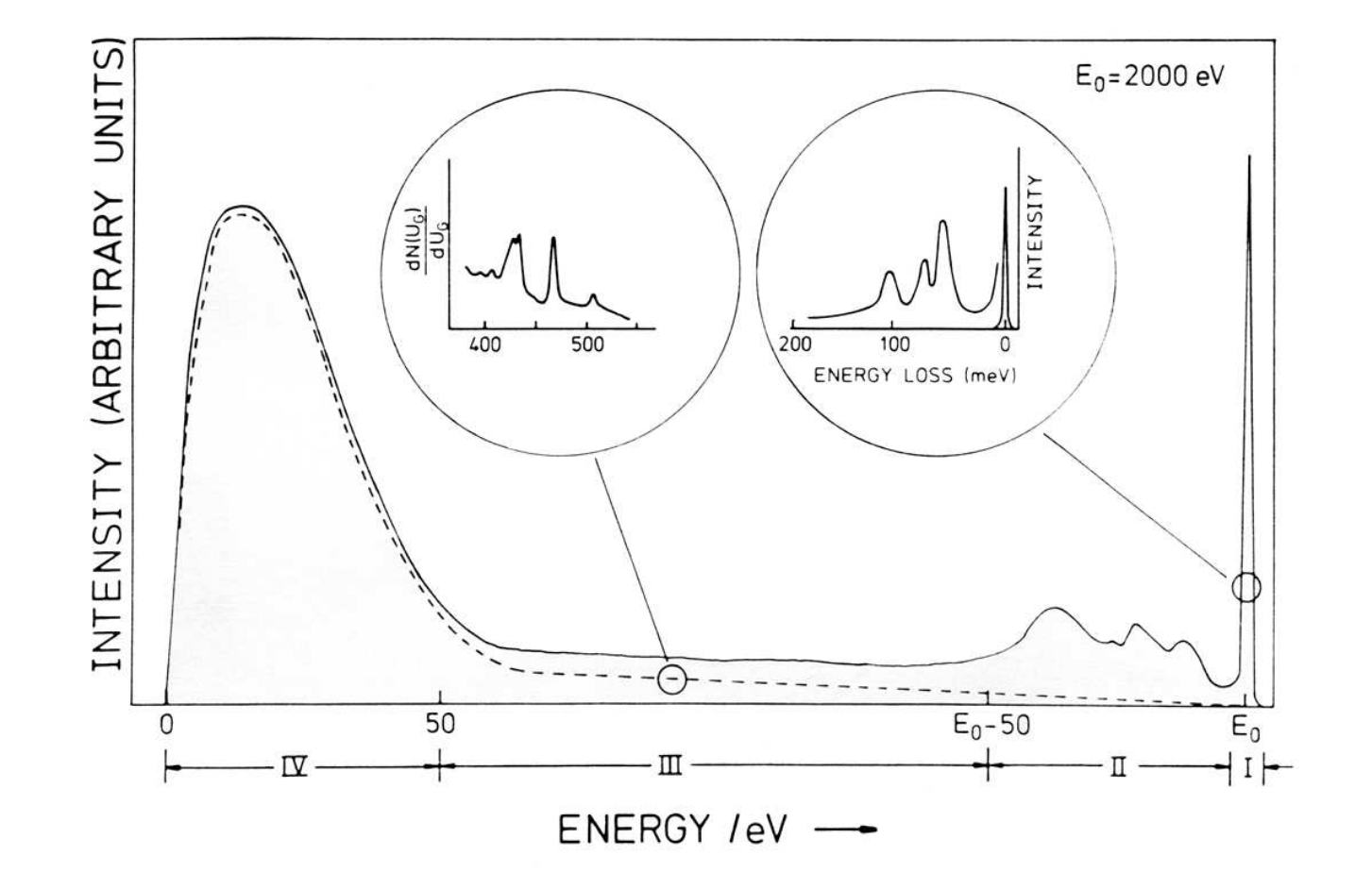

Problems...

Main issues in calculations of electron spectra for condensed matter applications:

- inclusion of the correlation: many interacting electrons causes unfavorable scaling:
  - $\exp(N)$ in general
  - N^6 in CISD
  - N^3 in QMC, DFT
- assessment of the band-like part of the spectra including shake phenomena
- extrinsic electron energy loss: escaping electrons may suffer inelastic collisions with surrounding electronic cloud and collective charge motion.

What can QMMC do?

- Computational tool for investigating properties of matter (from atoms to solids) by the interaction with projectiles (photons, electrons and ions).
- QMMC provides an extension of Fano's resonant multichannel scattering theory to condensed matter applications at cost comparable to that of molecules.
- QMMC calculates photoemission and non radiative decay spectra through:
  - Ab-initio: intrinsic features of a system (electronic structure, e/de-xcitation including accurate treatment of many-body effects)
  - Monte Carlo: extrinsic electron energy loss (inelastic and plasmon scattering energy loss)

The QMMC Method

The problem: from first principles, solve the scattering problem including the correlation effects and the proper boundary conditions, predict the cross sections and show how they compare with experimental measurements.

The QMMC Method

The problem: from first principles, solve the scattering problem including the correlation effects and the proper boundary conditions, predict the cross sections and show how they compare with experimental measurements.

- Splitting the problem into three parts:
  - System=cluster+environment
  - Electronic structure and continuum wavefunction calculations: peak position, intensity and lifetime of the resonance.
  - Superimpose electron energy loss using a Monte Carlo technique.

Electronic structure calculation

Splitting the problem:

MD+HF+ CI (HGF) → LS+Interchannel +SESP → Extraction of the observables

Molecular dynamics produces:

- relaxed geometrical structure.

Electronic structure calculations:

- HGF basis set.
- HF: All electron mean field treatment of the e-e interaction.
- CI: inclusion of the exchange-correlation.

produce: partial occupancies, band structure, access to excited states

The QMMC method

Cluster choice is a trade-off between computational cost and accuracy:

$N_{tot} = N_b + N_m + N_v$ = total number of HGF

N_b = total number of bi-occupied after HF

N_m = total number of mono-occupied orbitals after HF

N_v = total number of virtual orbitals after HF

$N_c = N_{b_c} + N_{v_c} + N_{m_c}$ = total number of cluster orbitals

The QMMC method

- The cluster functional space (N_c) is not orthogonal to neither bi-occupied (N_b) nor virtual (including bonding orbitals) ($N_m + N_v$) functional space of the all system (N) after HF: one needs to orthogonalize it to lower the computational cost.
- We separately diagonalize the bioccupied and virtual orbitals spaces by projecting into the cluster functional space through:

$$P_b = \sum_{ij=1}^{N_{b_c}} |g_i > S_{ij}^{-1} < g_j| \quad P_v = \sum_{ij=1}^{N_{v_c}} |g_i > S_{ij}^{-1} < g_j|$$

where

$$S_{ij}^{-1} =< g_i|g_j >$$

- This rotation makes no change in energy and total wavefunction
- Eigenvalue = 0 (1) means outside (inside) the cluster functional space, intermediate values means bonding orbitals

The QMMC method

	HGF System	HGF Cluster	HGF Environment
Total (Initial)	369	89	280
Bi-occupied orbitals	160	42	118
Mono-occupied orbitals	1	0	1
Virtuals+bonds orbitals	208	77	131

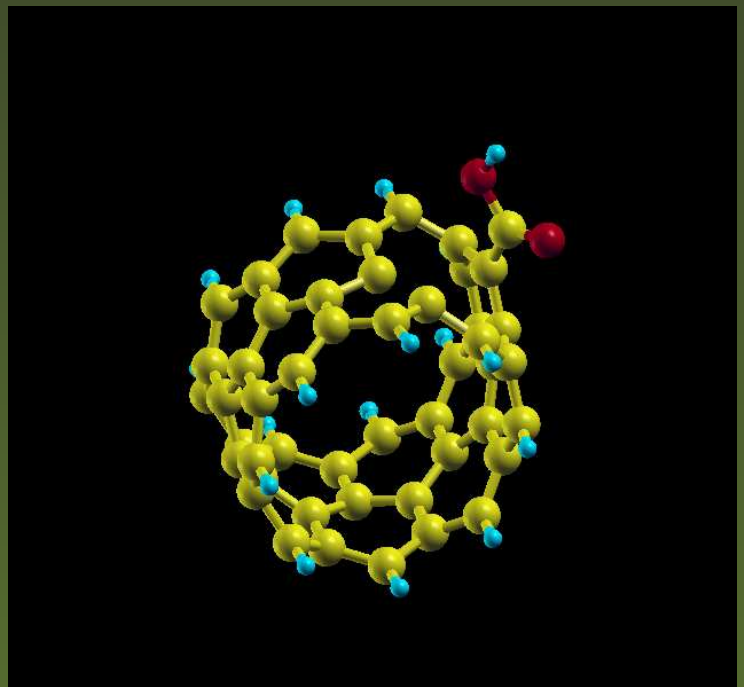

The QMMC method

The multichannel theory of scattering aims to find positive energy solutions of the many-body Hamiltonian:

$$(\hat{H} - E)\Psi^{-}_{\alpha,\epsilon} = 0$$

$$\hat{H}(1,..,N) = \sum_{i=1}^{N}[\hat{T}(i) + \hat{V}^{en}(i)] + \frac{1}{2}\sum_{i\neq j}^{N}\hat{v}(i,j) = \hat{H}_0 + \sum_{i\neq j}^{N}\hat{v}(i,j)$$

where:

$$\hat{T}(i) = -\frac{1}{2}\nabla_i^2; \quad \hat{V}^{en}(i) = \sum_{\mu}\frac{1}{|\mathbf{r}_i - \mathbf{R}_\mu|}, \quad \hat{v}(i,j) = \frac{1}{|\mathbf{r}_i - \mathbf{r}_j|}$$

For a multichannel process scattering wf has to include correlation among bound electrons in the final decay states of the system and between the double ion and the electron in the continuum.

The QMMC method

Scattering wavefunction of the electron ejected in the continuum in the long range limit:

$$\lim_{r_N \to \infty} \Psi^-_{\alpha,\epsilon}(1,2,...,N) \;\propto\; |\Theta_\alpha(1,2,...,N-1) > \;\; \left[|\sigma_\alpha(s_N)\, \psi^-_{\epsilon_\alpha}(\mathbf{r_N}) >\right]$$

$$+ |\sum_\beta \Theta_\beta(1,2,..,N-1) > \;\; \left[\sigma_\beta(s_N) \frac{e^{-i\theta_\beta}}{(2\pi)^{3/2}\; r_N}\right] \; S(\epsilon_\beta, \epsilon_\alpha)$$

where

$|\sigma_\alpha \psi^-_{\epsilon_\alpha} >$ = escaping electron spin-orbital

θ_β = phase shift

$S(\epsilon_\beta, \epsilon_\alpha)$ = scattering amplitudes coupling different channels

The QMMC method

Traditional way to solve with ingoing boundary conditions relies on the Static Exchange Approximation (SEA), which splits the scattering process in two steps:

HF for bound states

$$\hat{F}_\alpha^{(b)}\theta_i^\alpha(\mathbf{r}) = \varepsilon_i\theta_i^\alpha(\mathbf{r})$$

$$\hat{F}_\alpha^{(b)} = \hat{T} + \hat{V}_{en}(\mathbf{r}) + \sum_{j=1}^{N-2}\left[a_{\alpha j}^{(b)}\hat{J}_j^{(\alpha)}(\mathbf{r}) - c_{\alpha j}^{(b)}\hat{K}_j^{(\alpha)}(\mathbf{r})\right]$$

HF for continuum states

$$\hat{F}_\alpha^{(c)}|\psi_{\alpha\mathbf{k}}^-(\mathbf{r})>= \epsilon_\alpha|\psi_{\alpha\mathbf{k}}^-((\mathbf{r}))>$$

$$\hat{F}_\alpha^{(c)} = \hat{T} + \hat{V}_{en}(\mathbf{r}) + \sum_j\left[a_{\alpha j}^{(c)}\hat{J}_j^{(\alpha)}(\mathbf{r}) - c_{\alpha j}^{(c)}\hat{K}_j^{(\alpha)}(\mathbf{r})\right] = \hat{T} + \hat{V}_\alpha(\mathbf{r})$$

The QMMC method

Lippmann-Schwinger equation projected onto a model space:

$$\psi^-_{\alpha\mathbf{k}}(\mathbf{r}) = \phi_{\mathbf{k}}(\mathbf{r}) + \hat{G}^-_0(\epsilon_\alpha)\hat{\mathcal{T}}_\alpha(E)\phi_{\mathbf{k}}(\mathbf{r}) =$$
$$\phi_{\mathbf{k}}(\mathbf{r}) + \sum_{lj} < g_l|\hat{\mathcal{T}}_\alpha|g_j >< g_j|\phi_{\mathbf{k}} > \hat{G}^-_0(\epsilon_\alpha)|g_l >$$

$$\hat{\mathcal{T}}_\alpha = \hat{\mathcal{V}}^P_\alpha + \hat{\mathcal{V}}^P_\alpha G^-_0 \hat{\mathcal{T}}_\alpha$$

G^-_0, free single-particle Green's function at energy $\epsilon_\alpha = E - E_\alpha$ and $\hat{V}_\alpha$, screened projected Coulomb potential.

The structure of the scattering wavefunction in the asymptotic region suggests that the space $\mathcal{G}$ representing the scattering wavefunction in the interaction region can be chosen as:

$$\Psi_{\alpha\mathbf{k}_\alpha}(1,..N) = \sqrt{N}\,\hat{\mathcal{A}}\,\left[\,|\Theta_\alpha(1,...,N-1)\,\sigma_\alpha(s_N) >\ |\psi_{\vec{k}_\alpha}(\mathbf{r}_N) >\,\right]$$

where $\mathcal{A}$ = antisymmetrizer

The QMMC method

Interchannel interaction

$$< \Psi_{\beta\vec{p}_\beta}(1,..,N)|\, \hat{H} - E\, |\Psi_{\alpha\vec{k}_\alpha}(1,..,N) >= (2\pi)^3 \delta(\vec{k}-\vec{p})\delta_{\alpha\beta}(\frac{k^2}{2} + E_\alpha)$$
$$+ < \eta_{\vec{k}\alpha};\ \alpha|\hat{V}_\pi^{en}\delta_{\alpha\beta} + \hat{\mathcal{W}}_\pi^{\alpha\beta}|\eta_{\vec{p}\beta};\ \beta >$$

produces:

- decay probabilities correctly distributed among the open channels.
- electron-hole post-collisional interactions.

The QMMC method

Electronic structure calculations using Gaussians

scale as the 6th power of the system size ⇒ we need

ENERGY SPLIT TO TREAT EXTENDED SYSTEMS!!

Step 1 More intense transitions are selected ⇒ smaller Hamiltonian to diagonalize.

Step 2: Hole delocalization and band-effects enters by splitting previous interchannel states in a number of transitions close in energy and maximally overlapping with states selected in step 1

Physical observables

Within the frozen phonon approximation, for a photon beam polarized along the λ direction, first order perturbation theory gives for the Auger cross section

$$\frac{\partial\sigma_{0\to\alpha}}{\partial\vec{k}\partial\vec{p}}(\vec{k},\vec{p};\omega,\lambda) = (\frac{2\pi\omega}{c})\frac{|<0|\hat{O}_\lambda|\Psi^-_{\alpha,\epsilon_\alpha}>|^2}{E-E_r-i\frac{\Gamma}{2}}\Gamma_\alpha\delta(E_0+\hbar\omega-(E_\alpha+\frac{k^2+p^2}{2}))$$

where

- $\Gamma = \sum_\beta \Gamma_\beta = 2\pi\sum_\beta |M^-_\beta(\epsilon_\beta, E)|^2$
- $M^-_\beta(\epsilon_\beta, E) =< \Phi|H-E|\chi^-_{\beta,\epsilon_\beta} >$
- $|\Phi >$ = resonant core-hole intermediate state

Numerical issues...

S-wave scattering, comparison between hydrogenic (continuous line) and model (dashed line) solutions using s-type 50 tempered Gaussians

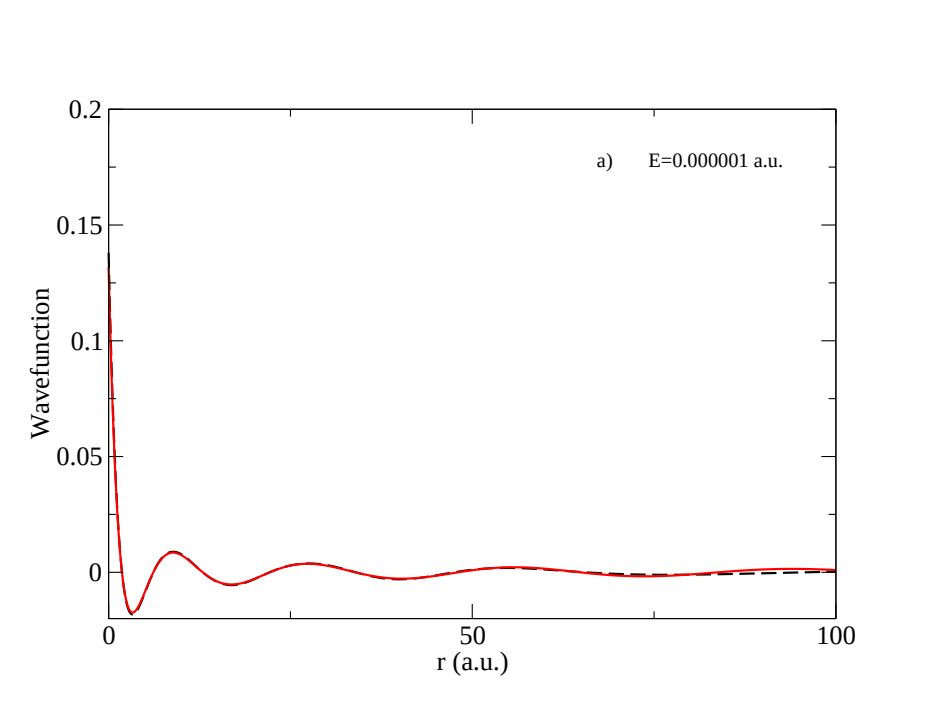

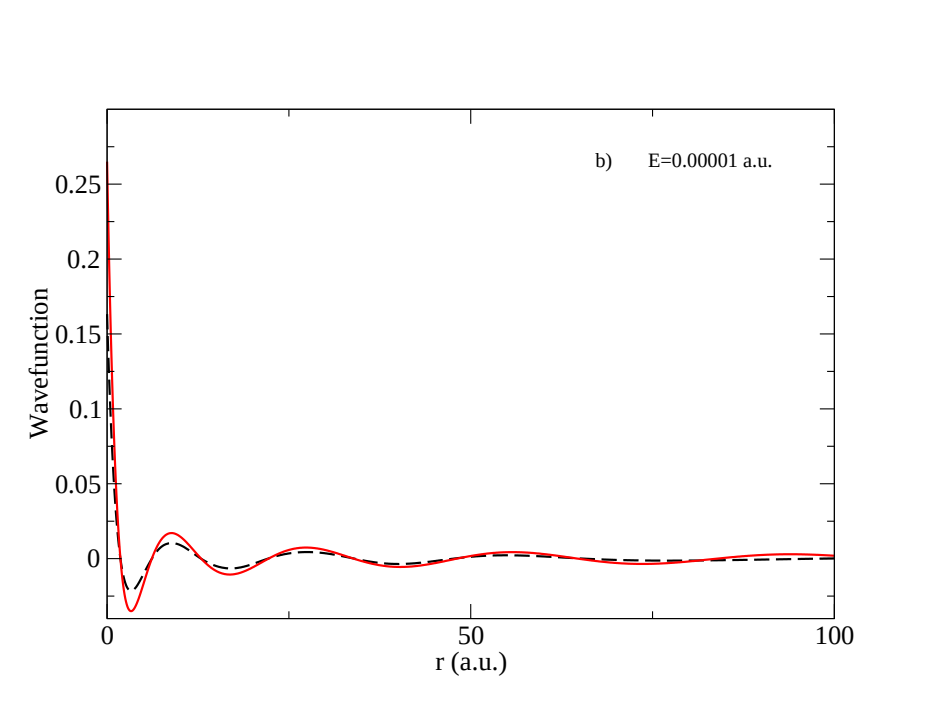

Numerical issues...

S-wave scattering, comparison between hydrogenic (continuous line) and model (dashed line) solutions using s-type 50 tempered Gaussians

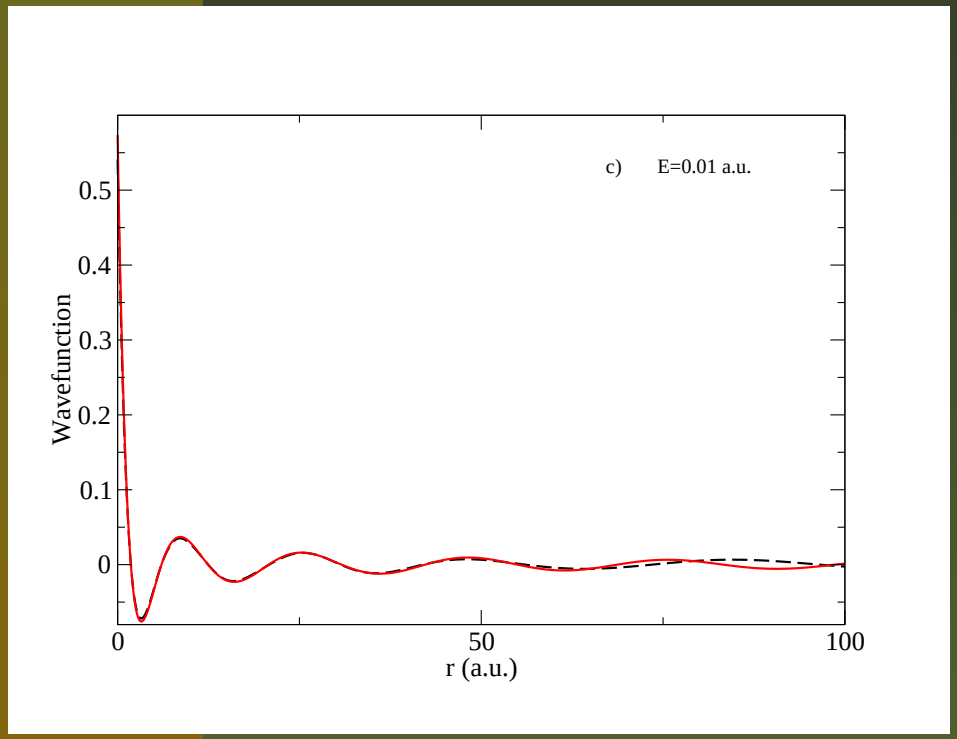

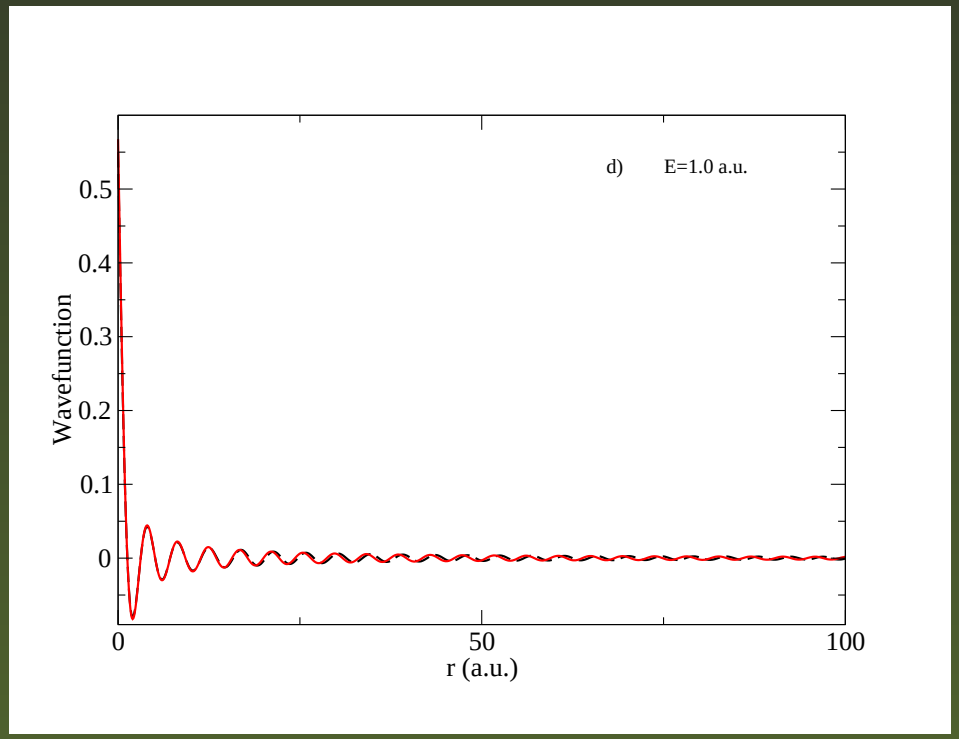

Numerical issues...

Comparison of exact hydrogenic (continuous-black line) and the model solution at 0.01 a.u. for different Gaussian numbers.

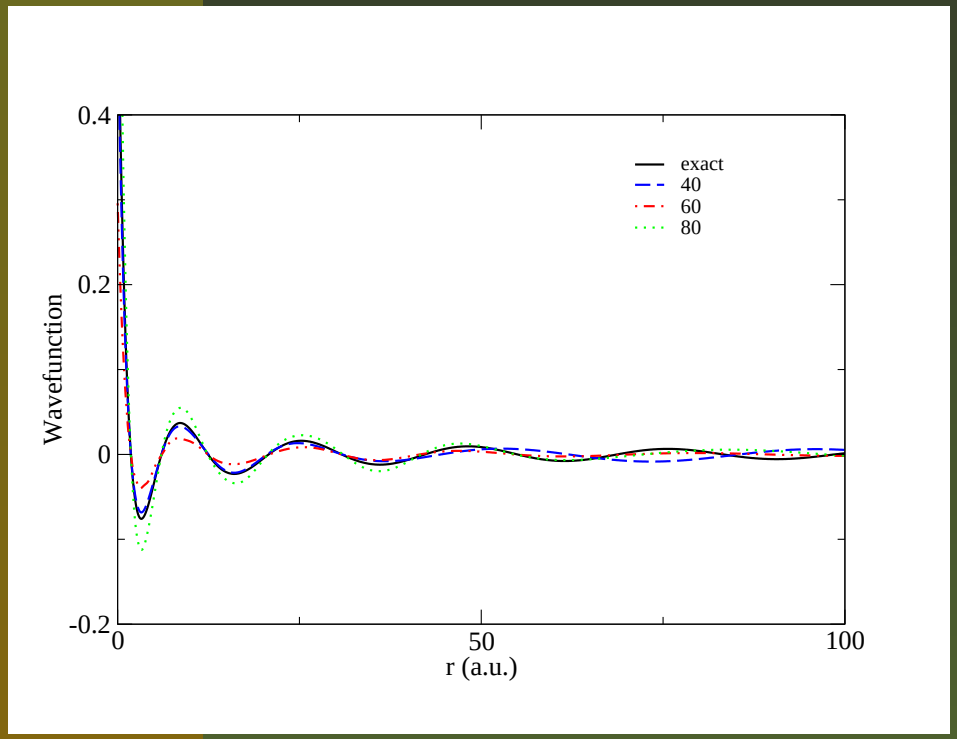

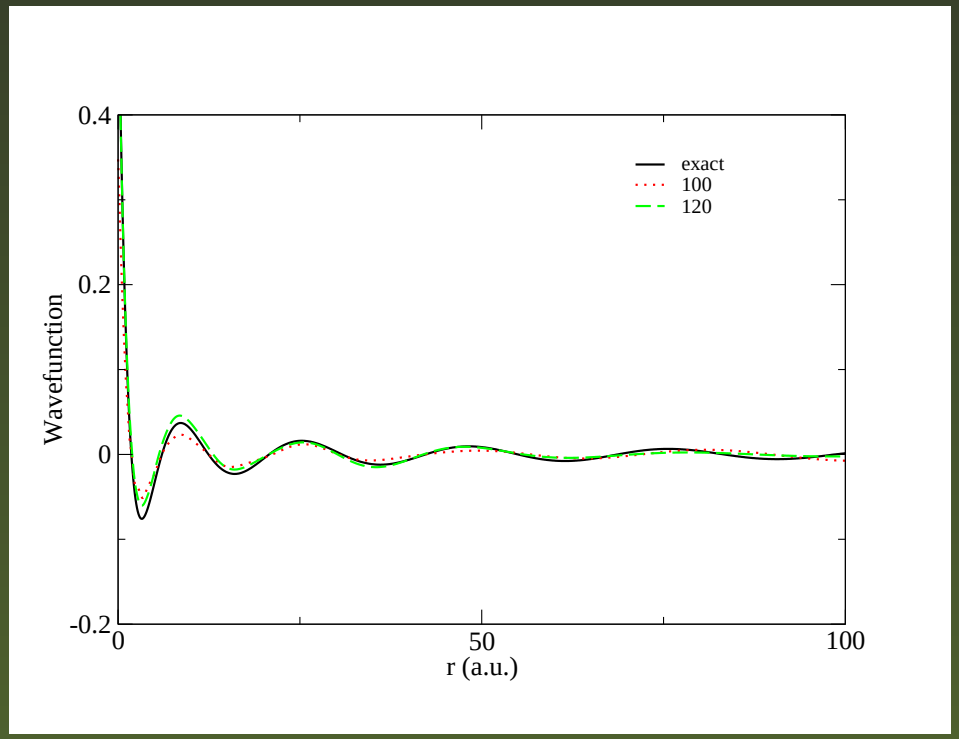

Scaling performances

- Concern is not only about the basis set but about the number of open channels as well.
- Gaussian basis set scales linearly with the number of atoms.
- Channels number scales as the second power
- Scattering potential needs a larger number of functions, approximately scaling linearly with the number of channels.
- Calculation of the interchannel potentials scales cubicly with the number of channels
- Symmetry may help in the calculation of the electronic correlation
- If symmetry halves the spanned functional space, Hamiltonian matrix cubic scaling inversions (Green operator) are eightfold reduced.

Monte Carlo energy loss

- Ab-initio Auger spectrum is the initial energy distribution of escaping electrons.
- The energy loss is a stochastic process.
- The step-length Δs is given by $\Delta s = -\lambda \ \ln(\mu_1)$, where
  - μ_1 is a random number uniformly distributed in $[0, 1]$.
  - λ is the electron mean free path:

$$\lambda(E) = \frac{1}{N[\sigma_{el}(E) + \sigma_{inel}(E)]} \ ,$$

  - N is the number of SiO_2 molecules per unit volume
  - $\sigma_{el}(E)$ is total elastic scattering cross section
  - $\sigma_{inel}(E)$ is the total inelastic scattering cross section
  - E = kinetic energy of an incident electron

Monte Carlo energy loss

- $\sigma_{el}(E)$ and $\frac{d\sigma_{el}(E,\omega)}{d\omega}$ are calculated via Relativistic Partial Wave Expansion method
- $\sigma_{inel}(E)$ and $\frac{d\sigma_{inel}(E,\omega)}{d\omega}$ are calculated via the Ritchie theory.

$$\frac{d\sigma_{inel}(E,\omega)}{d\omega} = \frac{me^2}{2\pi\hbar^2 NE}\mathrm{Im}\left[\frac{-1}{\varepsilon(\omega)}\right] S\left(\frac{\omega}{E}\right)$$

where

- ω is the energy loss
- The function S

$$S(x) = (1-x)\ln\frac{4}{x} - \frac{7}{4}x + x^{3/2} - \frac{33}{32}x^2 \ .$$

- $\varepsilon(\omega)$ is the long-wavelenght limit of the dielectric function.

Monte Carlo energy loss

- If ξ is a random variable in (a, b) with a given probability density $p(x)$, μ a variable uniformly distributed in $(0, 1)$, the values of ξ are related to those of μ by:

$$\int_a^{\xi} p(x)dx = \mu$$

- Uniform distribution in (a, b):

$$p_\eta(x) = \frac{1}{b-a}$$

If μ is a variable uniformly distributed in $(0, 1)$, then η:

$$\mu = \int_a^{\eta} p_\eta(x)dx = \mu = \int_a^{\eta} \frac{dx}{b-a}$$

$$\eta = a + \mu(b-a)$$

and its expected value

Monte Carlo energy loss

- Before each collision, a random number μ_2 uniformly distributed in $[0, 1]$ is generated and compared with $q_{inel} = \sigma_{inel}/(\sigma_{inel} + \sigma_{el})$.
- If $\mu_2 \leq q_{inel}$ collision is inelastic and energy loss W is computed via:

$$\mu_4 = \frac{1}{\sigma_{inel}} \int_0^W \frac{d\sigma_{inel}}{d\omega} d\omega \ ,$$

where

  - μ_4 is a random number uniformly distributed in $[0, 1]$:

Monte Carlo energy loss

- Before each collision, a random number μ_2 uniformly distributed in $[0, 1]$ is generated and compared with $q_{inel} = \sigma_{inel}/(\sigma_{inel} + \sigma_{el})$.
- If $\mu_2 \geq q_{inel}$ collision is elastic and the polar scattering angle, θ, is selected such that the random number μ_3 uniformly distributed in the range $[0, 1]$:

$$\mu_3 = \frac{1}{\sigma_{el}} \int_0^{\theta} \frac{d\sigma_{el}}{d\Omega} \, 2\pi \, \sin\vartheta \, d\vartheta \, ,$$

where

  - μ_3 is uniformly distributed in $[0, 1]$
  - Ω is the solid angle of scattering

Logical flow in QMMC

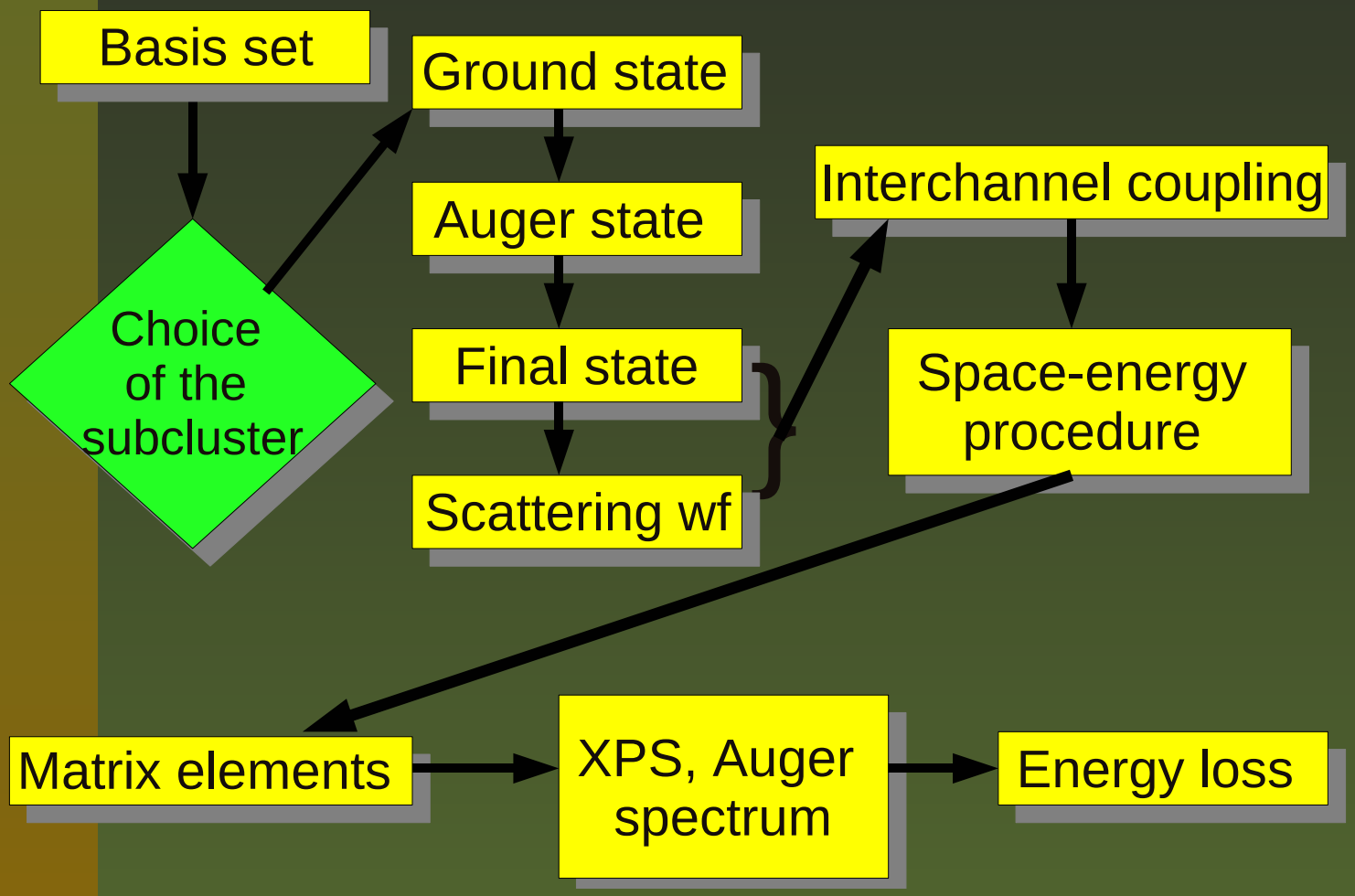

O $K - LL$ Auger spectra in SiO_2

Quantum Mechanical theoretical data (continuous line), the Monte Carlo results (dashed line) and the experimental data (point line).

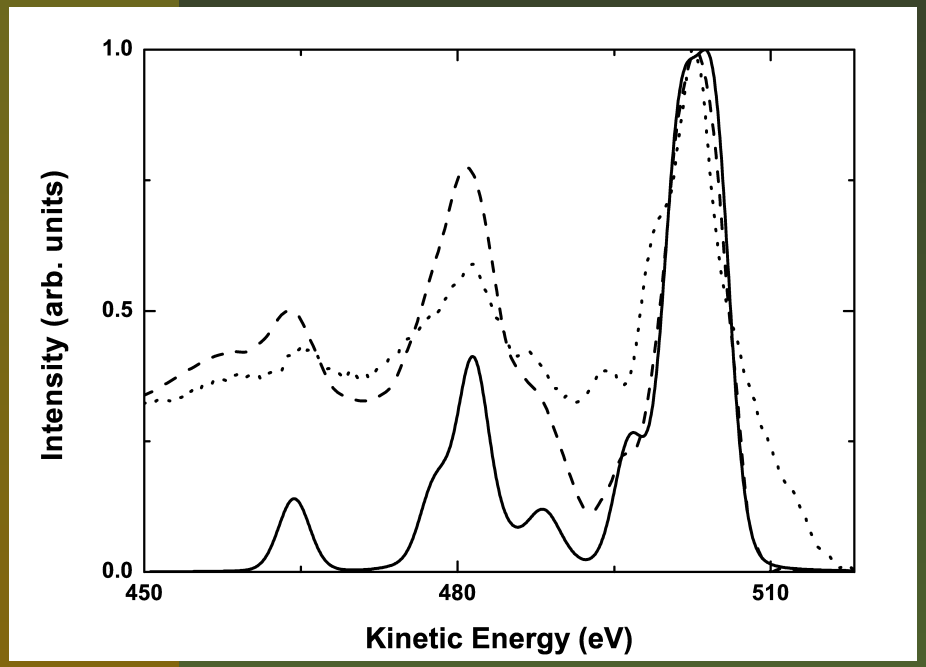

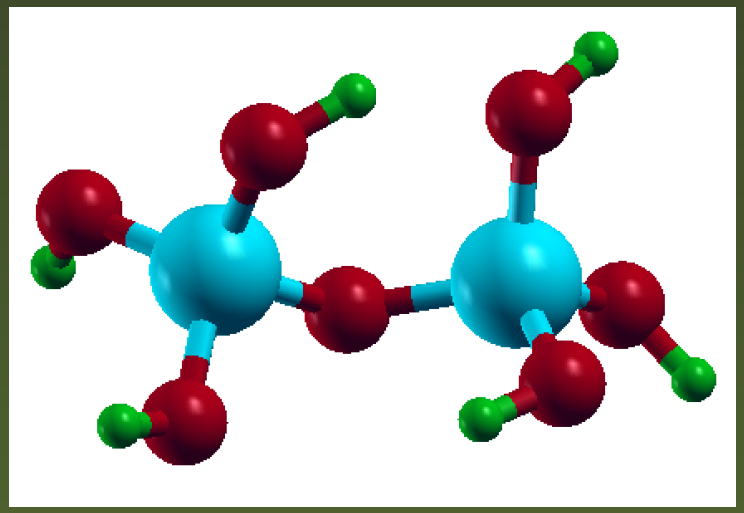

O/Si $K - LL$ Auger spectra in SiO_2

O K-LL	S^2	E_{kin}	Γ_α	Si K-LL	S^2	E_{kin}	Γ_α
$2s - 2s$	(0)	458.75	0.570	$2s - 2s$	(0)	1499.99	0.335
$2s - 2p$	(0)	473.4	0.511	$2s - 2p$	(0)	1544.66	0.860
$2s - 2p$	(0)	477.41	0.653	$2s - 2p$	(1)	1563.35	0.226
$2s - 2p$	(0)	477.99	0.624	$2p - 2p$	(0)	1598.19	0.362
$2s - 2p$	(1)	481.64	0.156	$2p - 2p$	(0)	1603.72	0.998
$2s - 2p$	(1)	484.96	0.182	$2p - 2p$	(0)	1603.73	1
$2s - 2p$	(1)	485.73	0.190	$2p - 2p$	(0)	1661.11	0.051
$2p - 2p$	(0)	493.94	0.670	$2p - 2p$	(0)	1714.15	0.039
$2p - 2p$	(0)	497.89	0.801	$2p - 2p$	(0)	1716.26	0.404
$2p - 2p$	(0)	498.74	0.862				
$2p - 2p$	(0)	500.28	0.829				

Si K – LL Auger spectra in SiO_2

Quantum mechanical calculation (continuous line), Monte Carlo results for different SiO2 layer thickness: 5 nm (dashed line), 10 nm (spaced point line), 15 nm (point-dashed line), 20 nm (small-dashed line), 25 nm (point line).

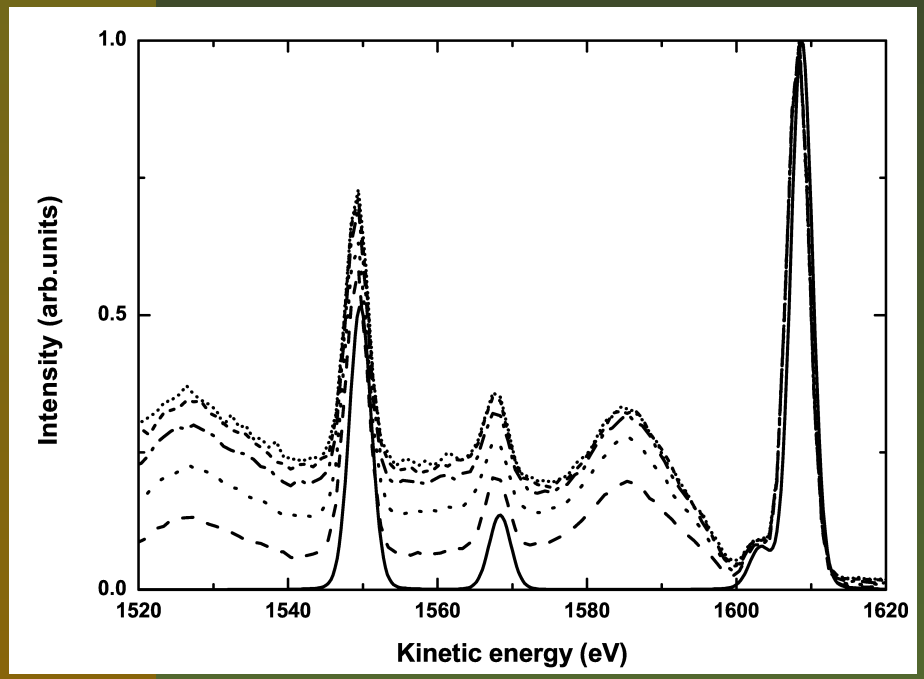

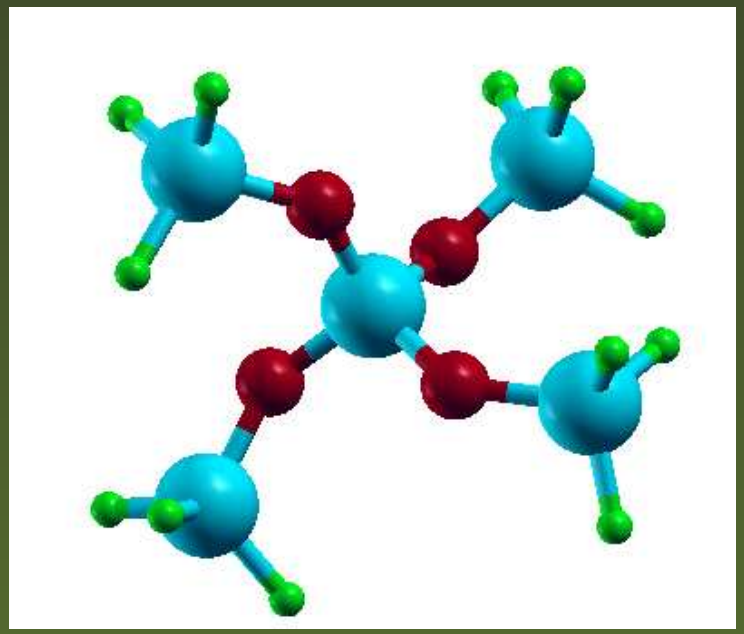

Tunable band-gap in qfs graphene

- The use of graphene in semiconductor devices requires a bandgap in order to switch the conductivity between an on and off state.
- Size quantization of about 1 nm induces band gaps of â$\frac{1}{4}$1 eV in graphene nanoribbons, CNT and quantum dots.
- However, in the case of nanotubes, the preparation of samples with ohmic contacts is still challenging. Similarly, in the case of nanoribbons, the electronic properties are determined by the edges, rendering this approach technologically very demanding.
- An alternative strategy is the chemical functionalization of graphene which induces bandgaps and can even be reversed.

Tunable band-gap in qfs graphene

- Hydrogenated amorphous carbon (a-C:H) has an optical gap increasing with the hydrogen content. Fully hydrogenated graphene, also referred to as graphane, has been suggested recently as an insulator with a bandgap of 3.5 eV.
- Hydrogenated graphene on SiC was investigated and found at H coverages of $\sim 1\%$, suggesting an electron localization as the mechanism responsible for the MIT.
- However, graphene on SiC is intrinsically heavily electron doped (EF is ~ 0.5 eV above the Dirac point) and as such is not the model system to be compared to the transport experiments on cleaved graphene.

Growth model of graphene

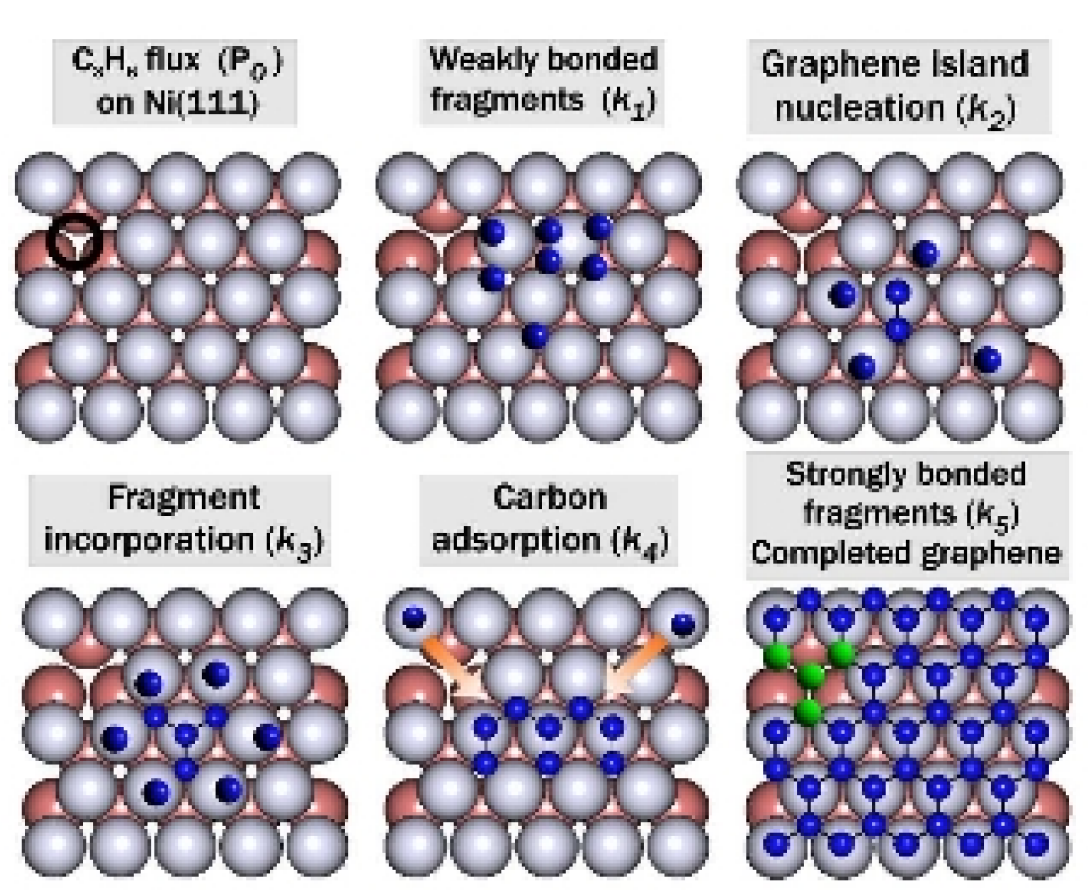

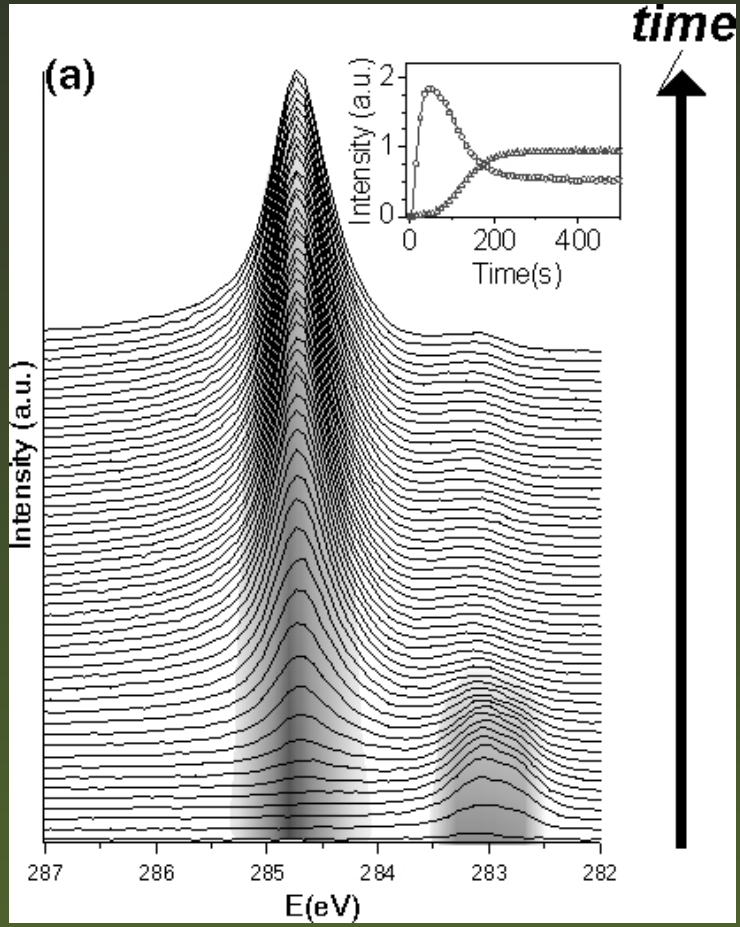

Propene C1s and EELS spectra

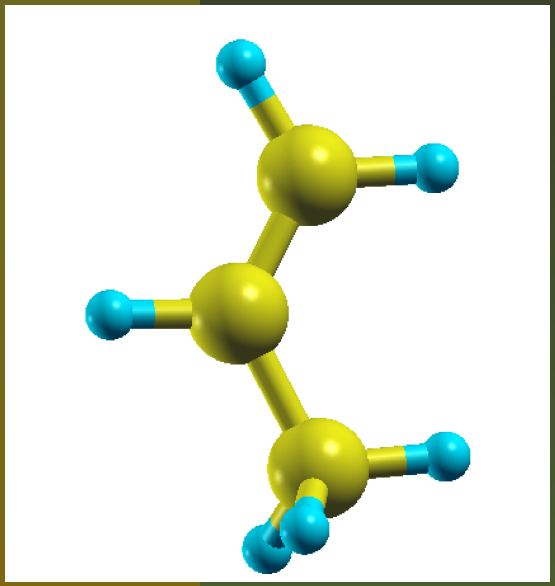

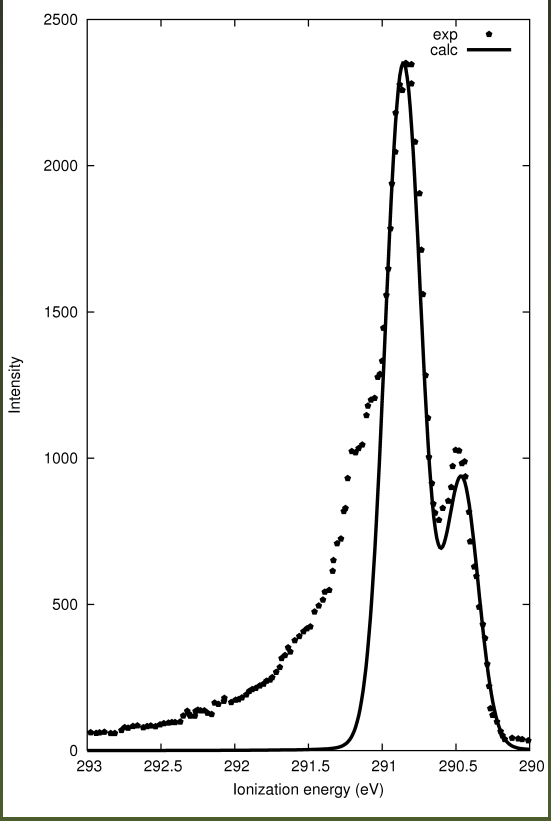

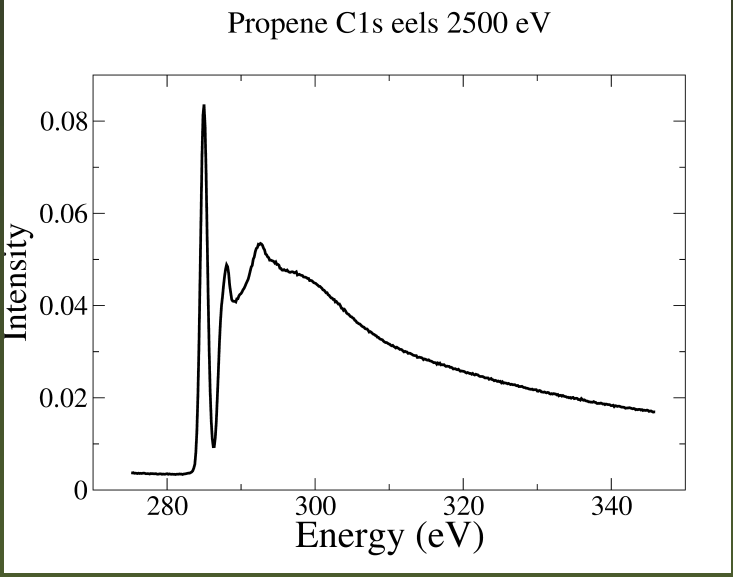

Growth model of graphene

C-Ni = 1.87 Å, C-H = 1.098 Å, $\widehat{C-H}$ = 109.4 °

C-Ni3 = 1.75 Å, C-H = 1.11 Å, $\widehat{C-Ni}$ = 91.5 °

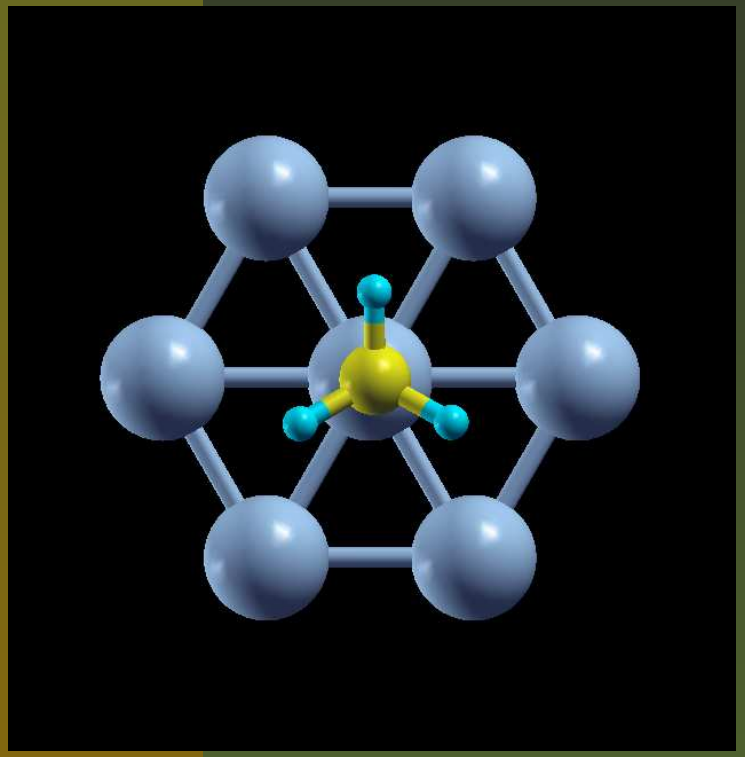

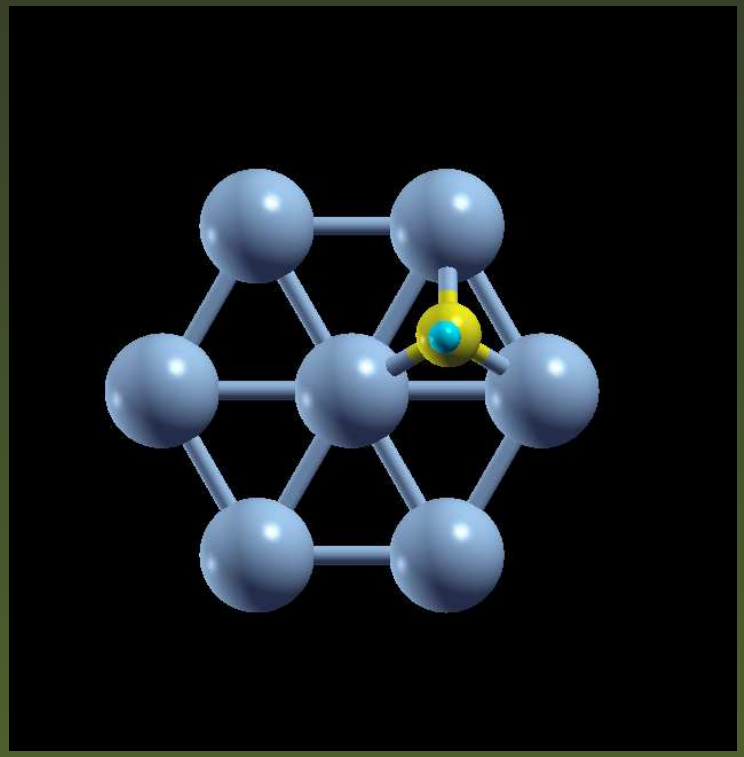

Growth model of graphene

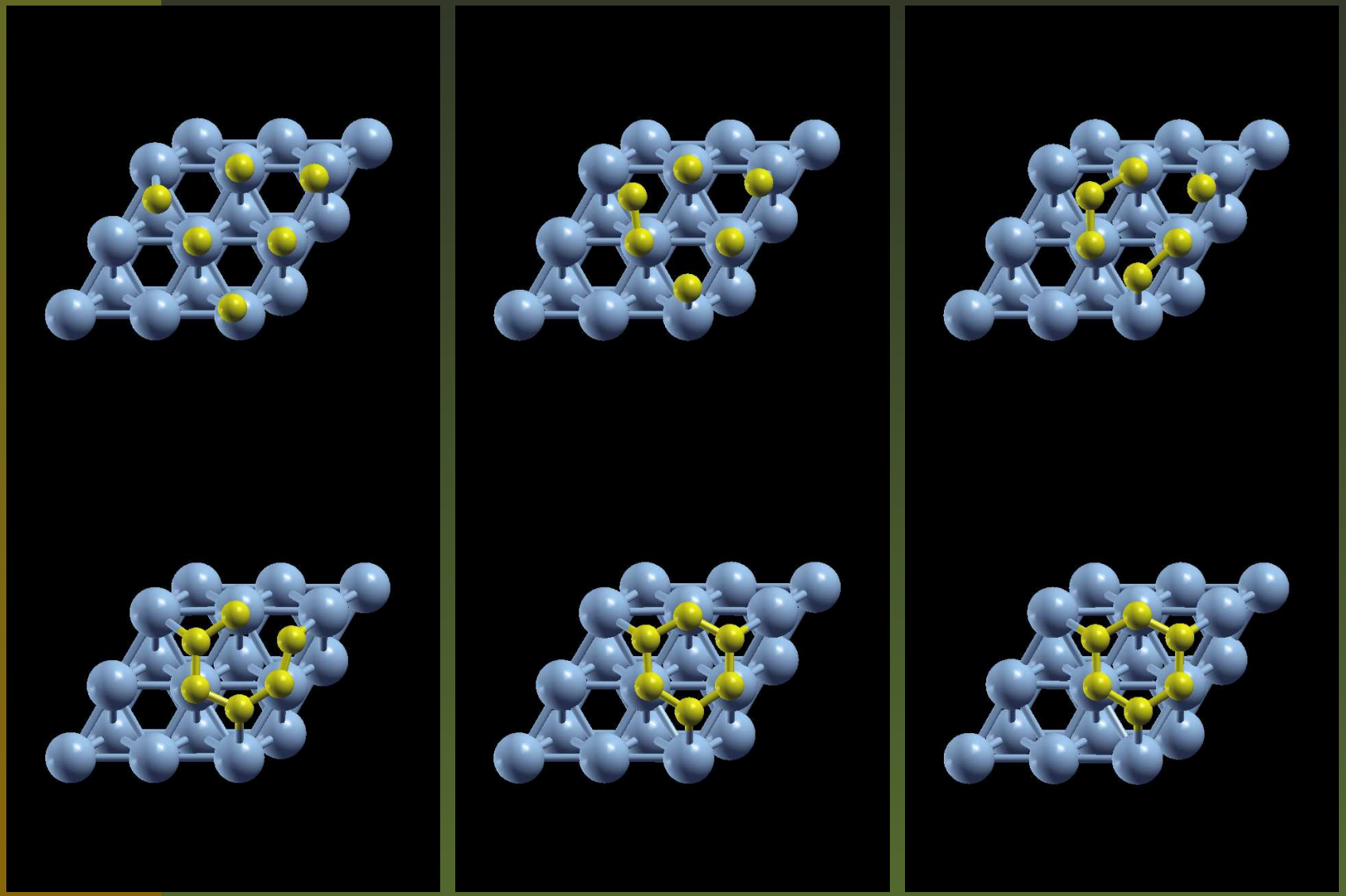

Growth model of graphene

40 a.u., 160 a.u (kinetic energy and charge cut-offs), forces < 0.001 eV Å per atom

LDA: C-Ni = 2.08 Å, C-Ni = 2.11 Å, C-C = 1.43 Å, Ni-Ni = 2.49 Å

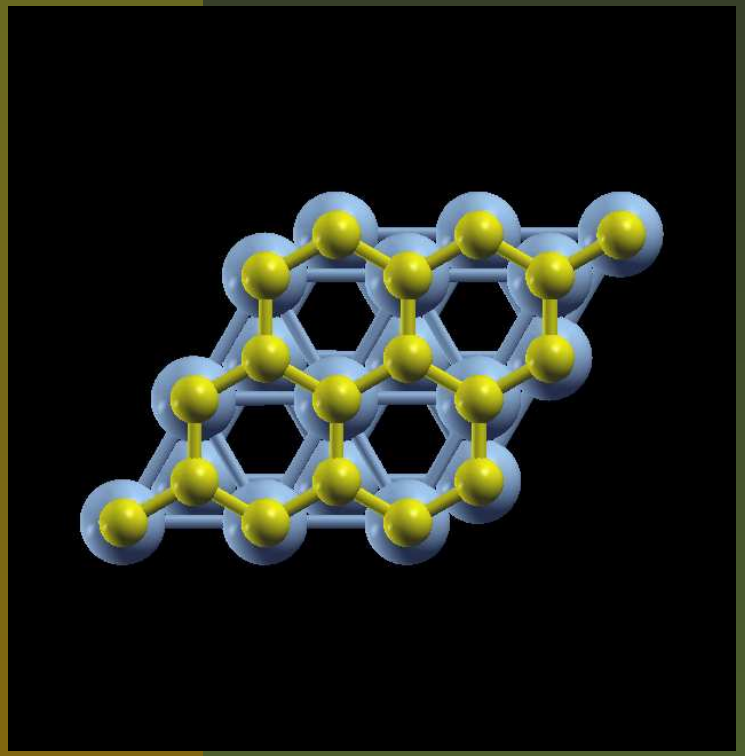

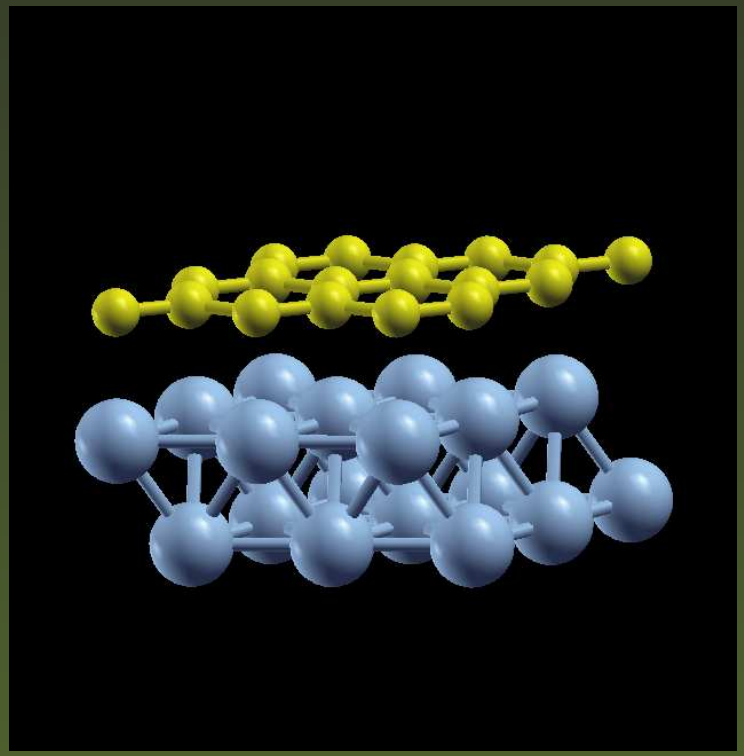

Tunable band-gap in qfs graphene

- By ARPES we find a tunable gap in q.f.s. graphene on Au induced by hydrogenation (MIT).
- Local rehybridization from sp^2 to sp^3 is observed by XPS and EXAFS allowing a determination of the chemisorbed hydrogen amount.
- Hydrogen induced gap formation is completely reversible by annealing without damaging the graphene.
- The size of the gap can be controlled via hydrogen loading and reaches $\sim$ 1.0 eV for a hydrogen coverage of 8%.
- Hydrogenation of graphene gives access to tunable electronic and optical properties and thereby provides a model system to study hydrogen storage in carbon materials.

XPS: $h\nu$= 380 eV, res = 50 meV

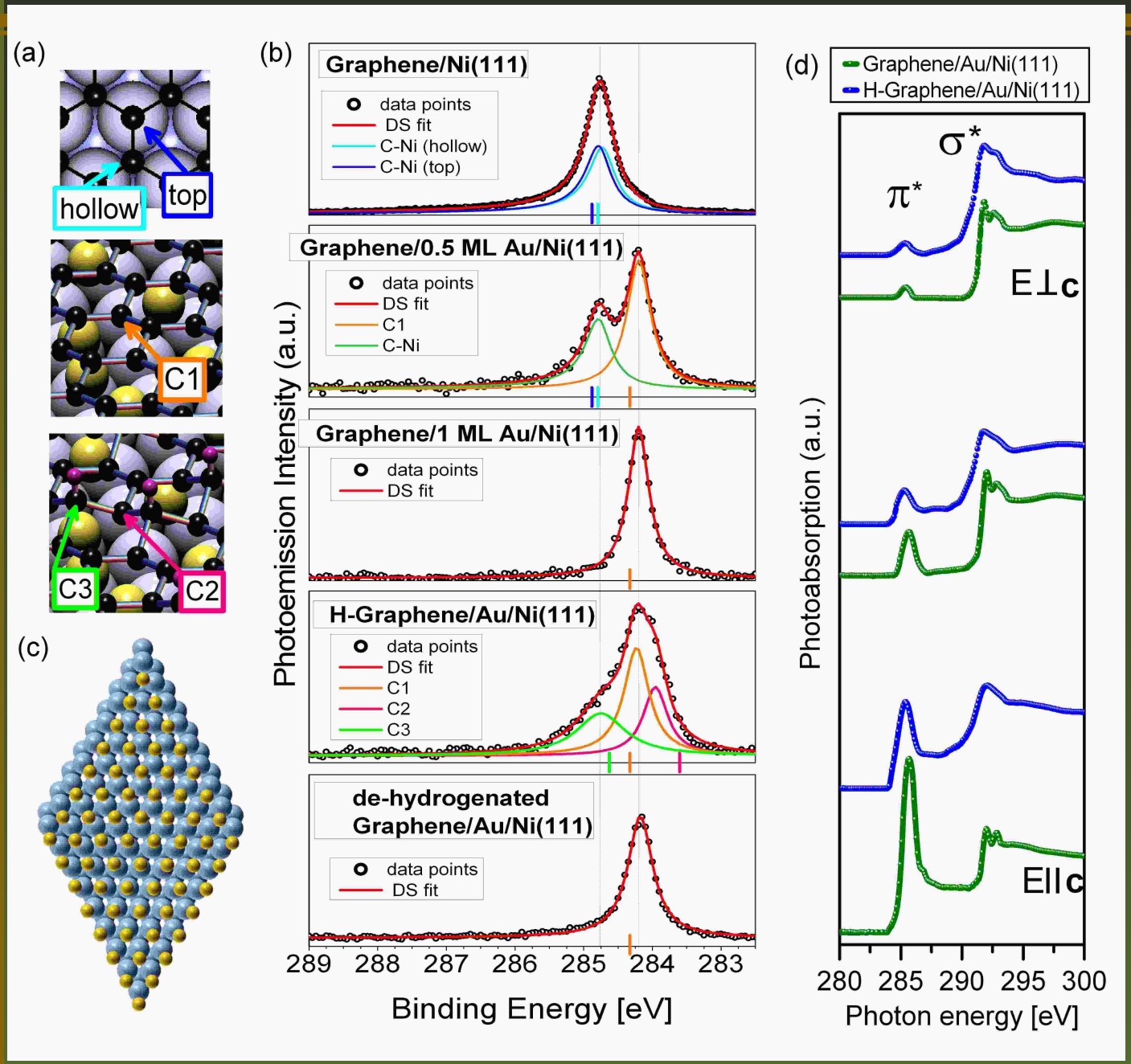

Theoretical results

$[19s(=10s_{Ni}+7s_C+2s_H)+15p=9p_{Ni}+5p_C+1p_H)+6d(=5d_{Ni}+1d_C)]$

System	top(exp)	hollow(exp)	2nd floor
Ni(111)-graphene(lda)	284.8 (284.7)	284.89 (284.8)	
Ni(111)-CH $(wf)_3$	288.23		
Ni(111)-CH (wf)	288.29		
Ni(111)-graph-CH_3(wf)			290.24
System	C1(exp)	C2(exp)	C3(exp)
H-graphene/Au	284.2(284.33)	283.9(283.59)	284.7(284.61)

ARPES: hν = 40.8 eV, AR=0.3°

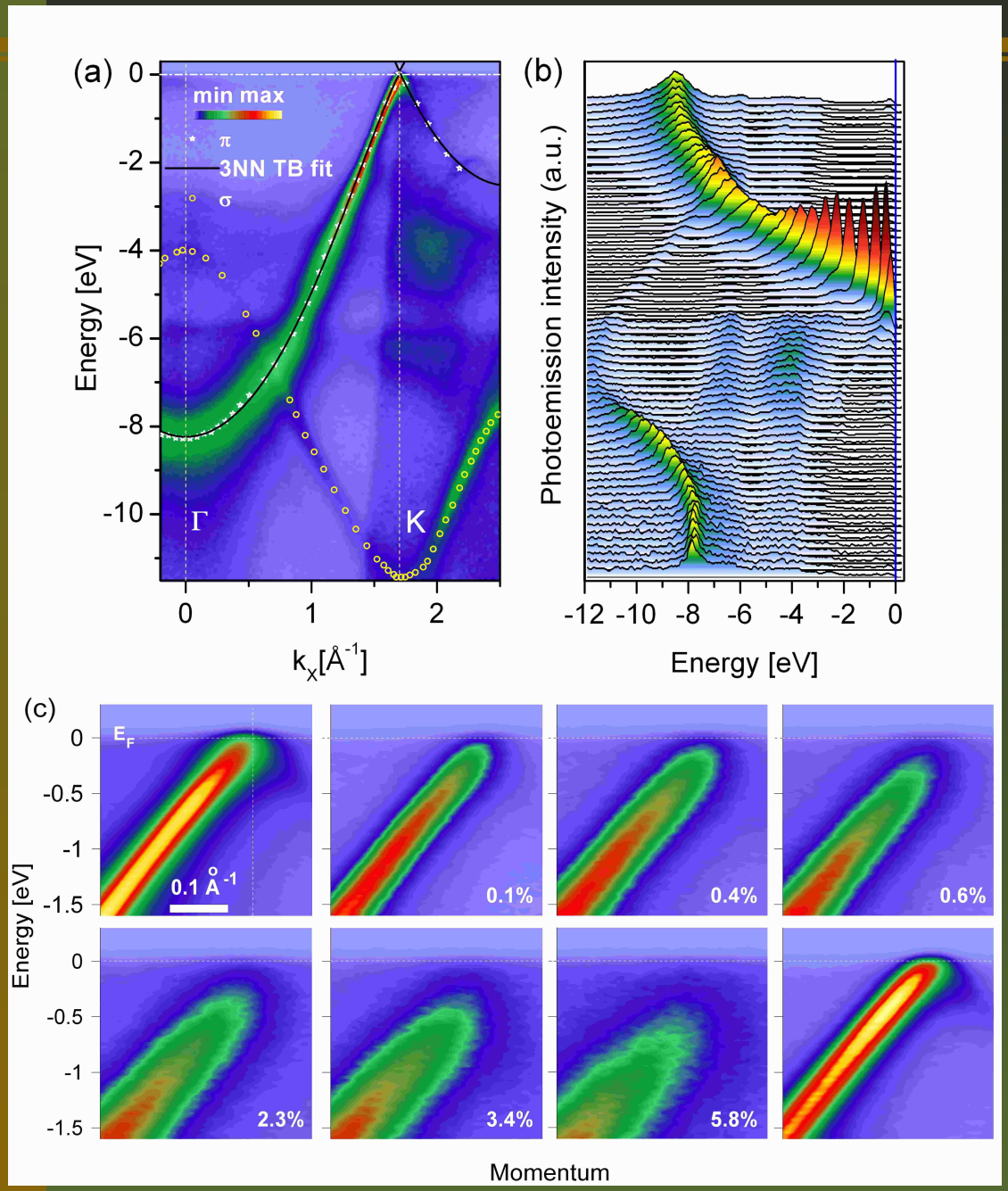

XPS and ARPES results

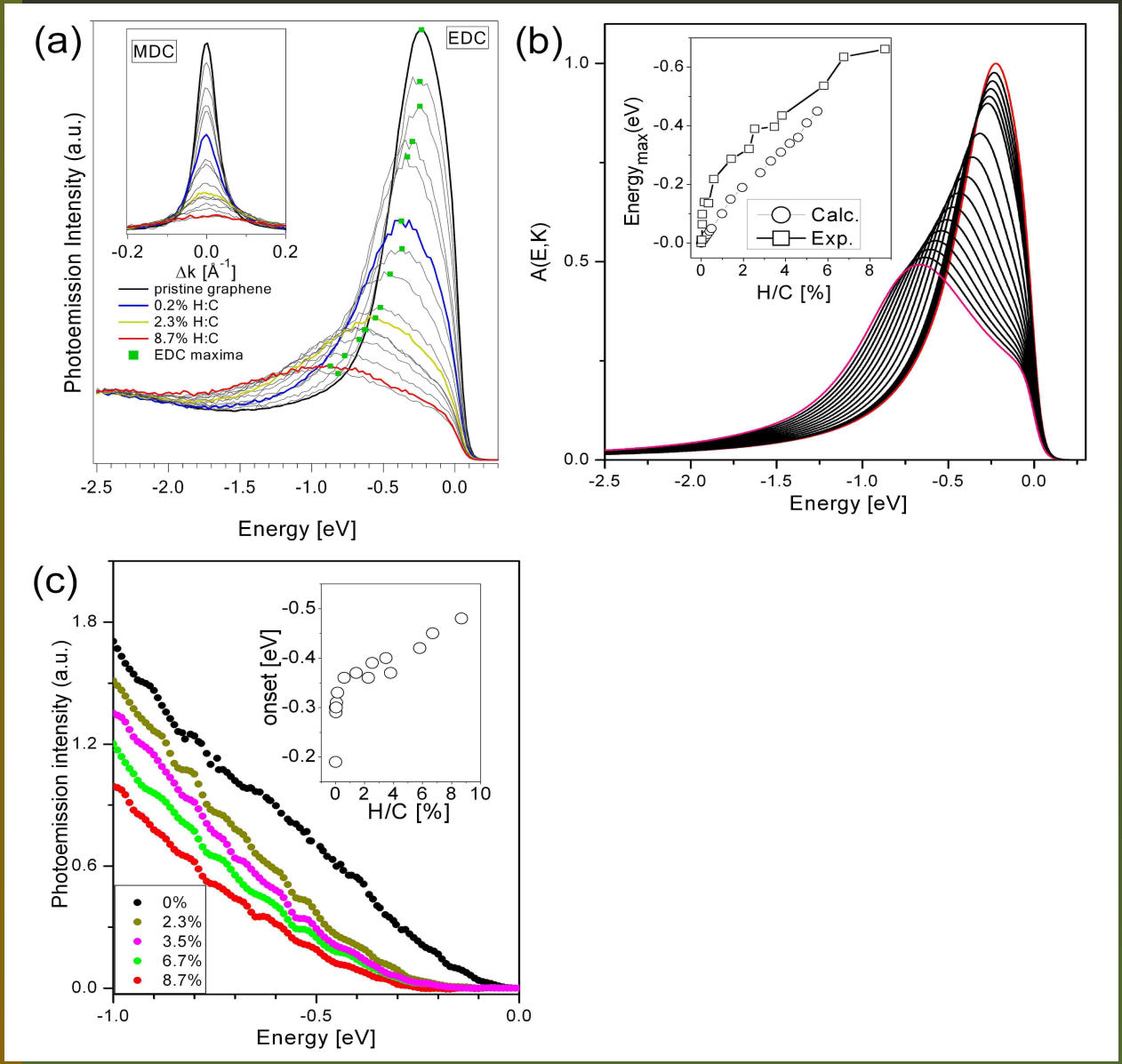

First conclusions

- C_{1s} core level shift of 0.5 eV towards lower binding energy upon Au intercalation in between the graphene/Ni(111) interface, resulting in a substantial reduction of the substrate interaction.
- This is in accordance with our calculations that predict a reduction of the cohesive energy per atom by 0.4 eV and an increase of the graphene-substrate distance by 1 Å.
- The exposure of graphene to atomic hydrogen induces the formation of C-H bonds resulting in a local sp^3 hybridization. This is directly observed in XPS by the appearance of two additional C1s peaks, separated by almost 1eV, originating from the C-H bond and the C atom next to it.
- NEXAFS measurements indicate a rehybridization from sp^2 to sp^3 and the formation of C-H bonds perpendicular to the graphene layer.

First conclusions

- Most importantly, the ARPES spectra of hydrogenated graphene clearly show the downshift of the π bandâs spectral function to lower energies and also a broadening.
- Our calculations support sublattice symmetry breaking as the reason for the observed changes in the ARPES upon hydrogenation.
- Tunability

Growth model of graphene

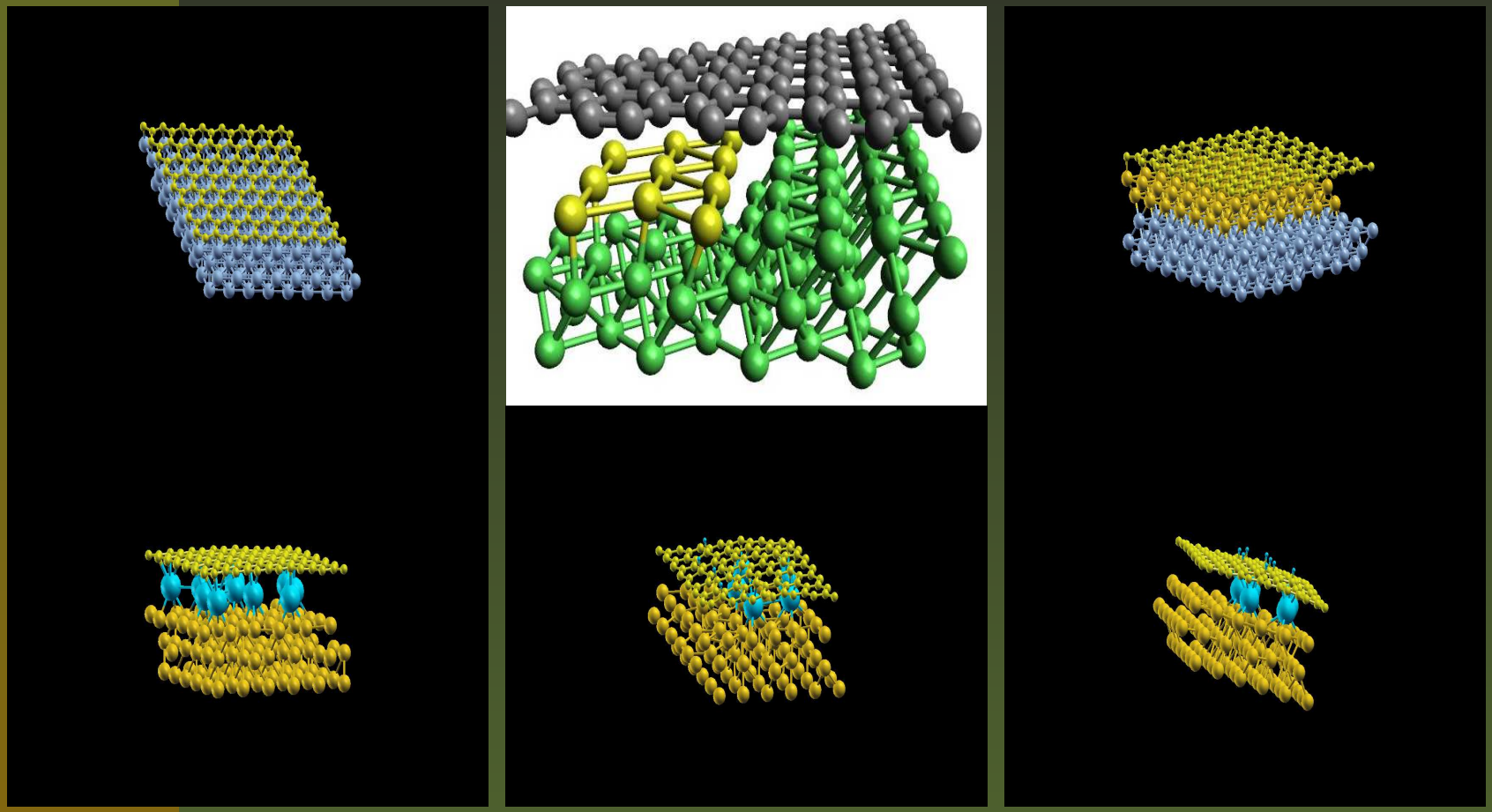

ARPES: hν = 40.8 eV, AR=0.3°

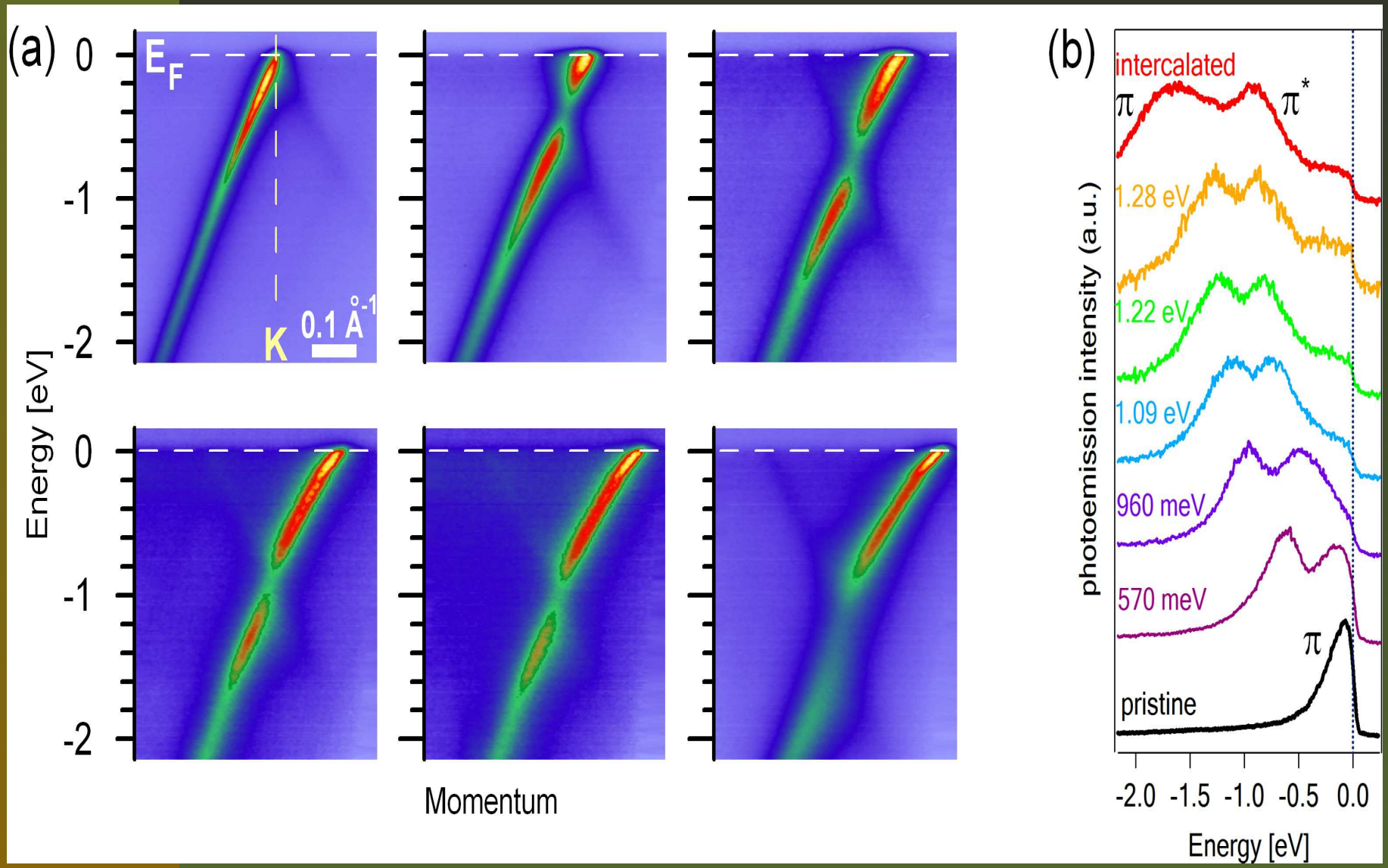

ARPES again

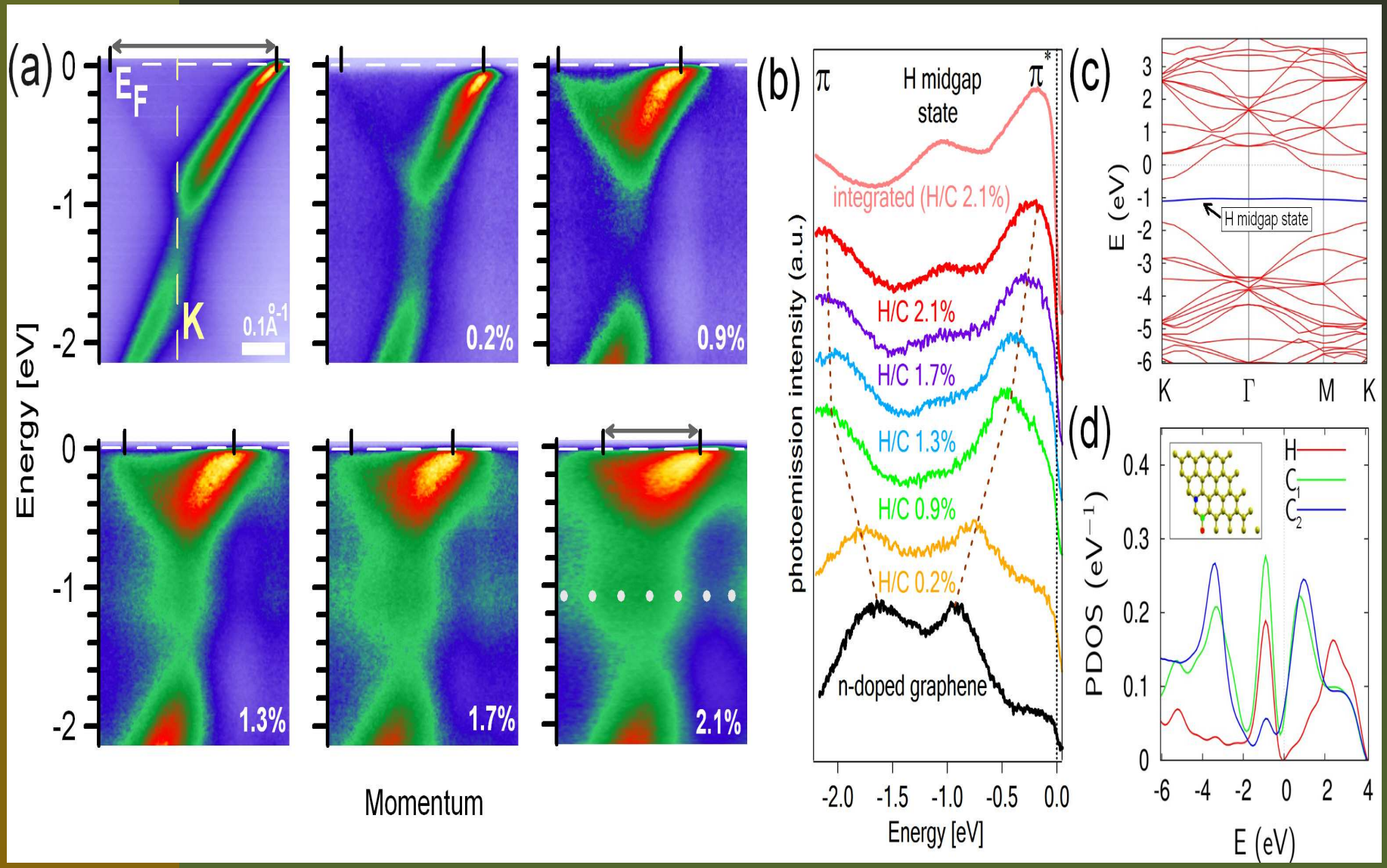
(a)
E_F
K
0.1Å^{-1}
0.2%
0.9%
1.3%
1.7%
2.1%
Energy [eV]
Momentum
(b)
π
H midgap state
π*
integrated (H/C 2.1%)
H/C 2.1%
H/C 1.7%
H/C 1.3%
H/C 0.9%
H/C 0.2%
n-doped graphene
photoemission intensity (a.u.)
Energy [eV]
(c)
H midgap state
E (eV)
K
Γ
M
K
(d)
H
C_1
C_2
PDOS (eV^{-1})
E (eV)

Deep acceptor level in H-graphene

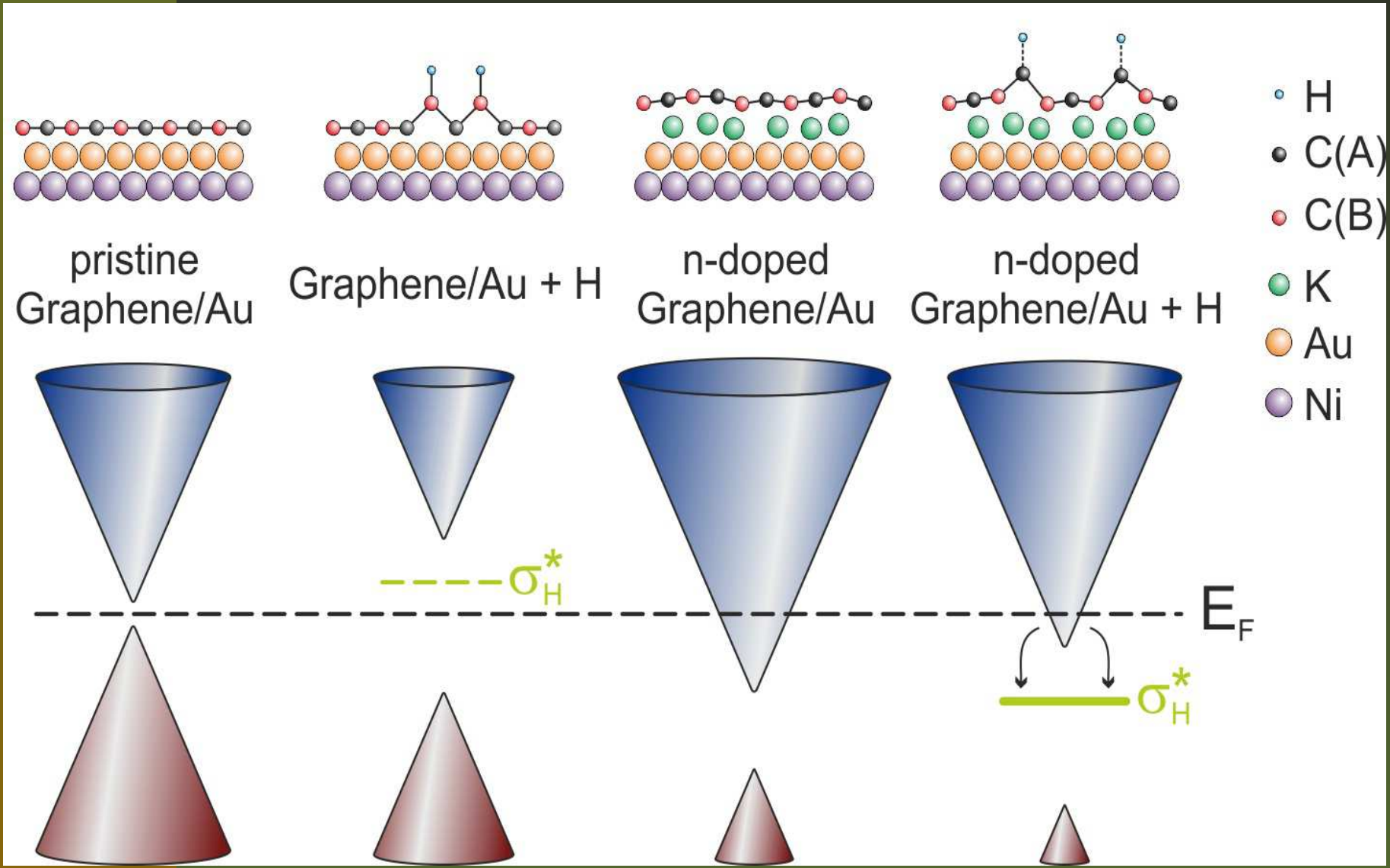

PDOS

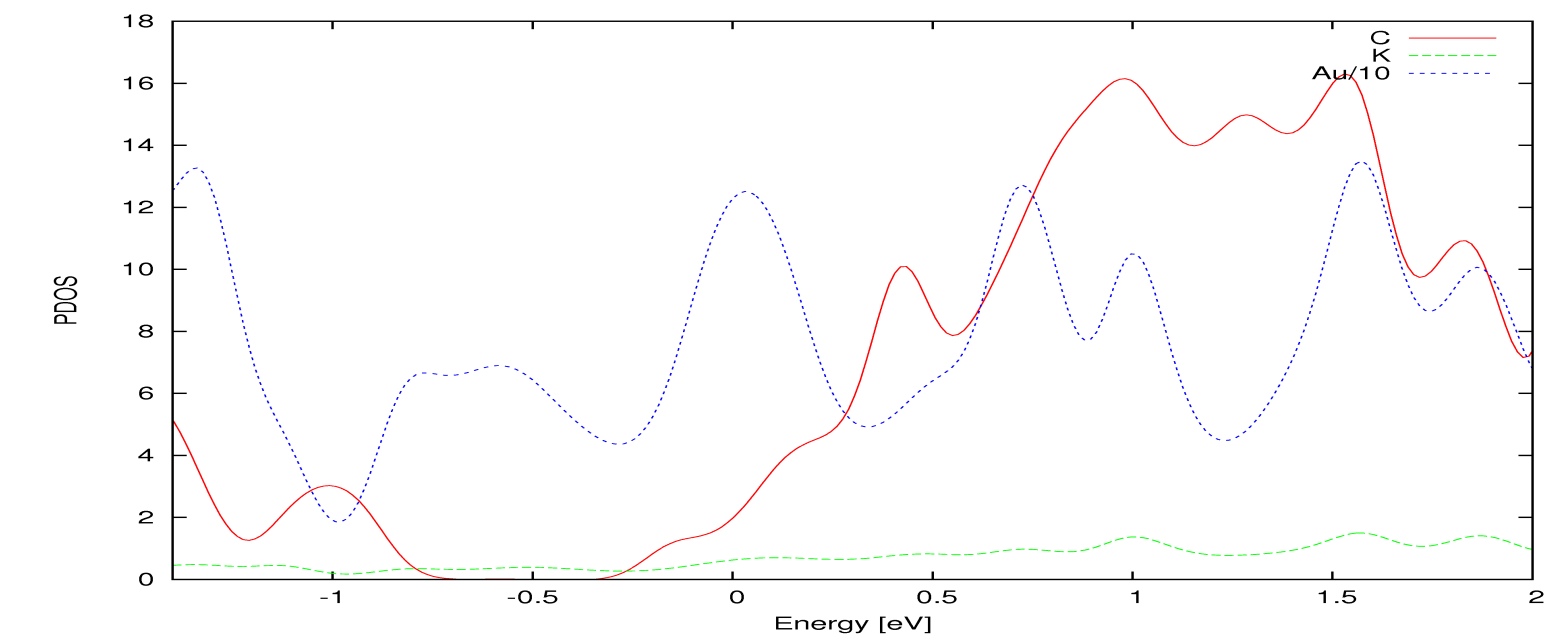
PDOS
Energy [eV]
C
K
Au/10
0
2
4
6
8
10
12
14
16
18
-1
-0.5
0
0.5
1
1.5
2

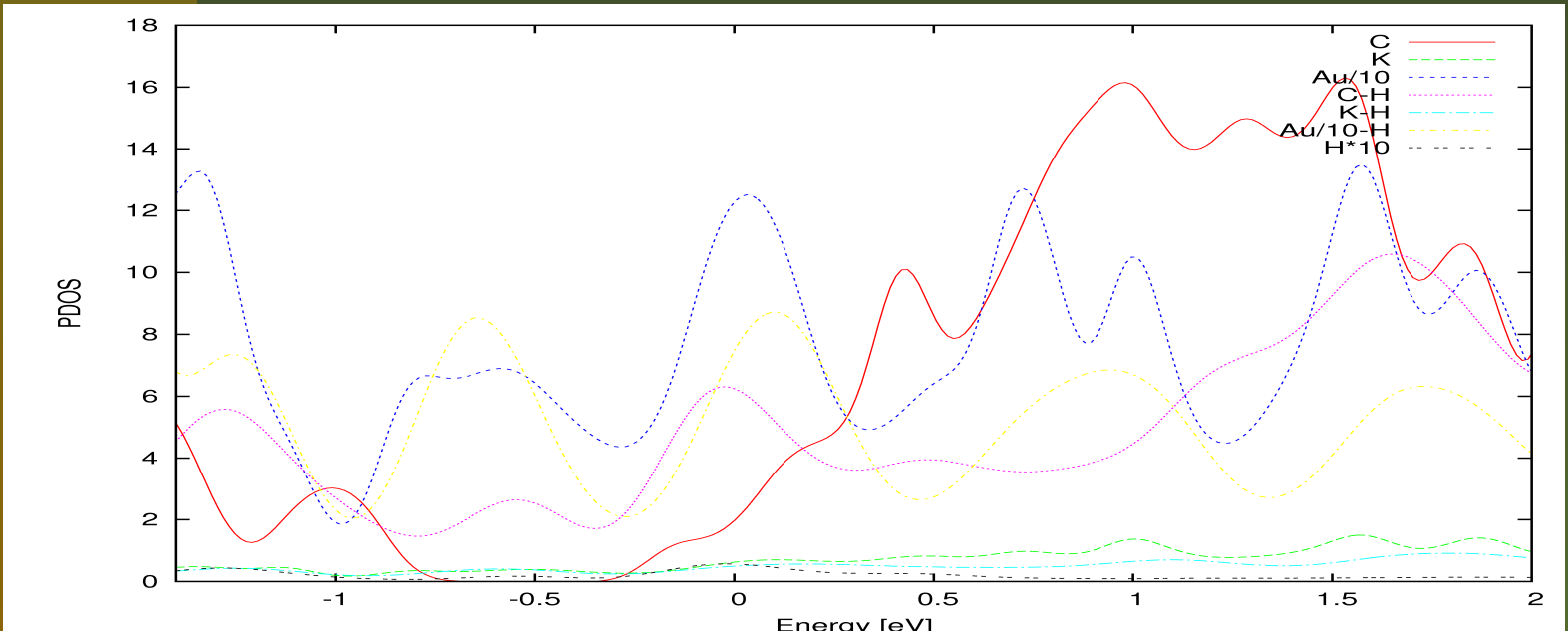
PDOS
Energy [eV]
C
K
Au/10
C-H
K-H
Au/10-H
H*10
0
2
4
6
8
10
12
14
16
18
-1
-0.5
0
0.5
1
1.5
2

Second conclusions

- Hydrogenated graphene has an acceptor level and the electron concen- tration in graphene can be controlled via the H/C ratio.
- DFT calculations of the DOS show this band to be largely composed from H 1s orbitals.
- An estimation of the Mott criterion and the calculation of the typical DOS suggests that the impurity band is stable against randomness in the H chemisorption and remains extended.
- The narrow acceptor level found in our ARPES data is ex- pected to give rise to metallic conduction when the chem- ical potential is tuned to cross the impurity band. The small bandwidth of this band makes it a strongly corre- lated band, dominantly derived from hydrogenic s bands.
- Electron doping of H-graphene could represent a route to form metallic bands from Hydrogen 1s states for high-Tc superconductors in alternative to solid hydrogen which requires extremely high pressures.

Take home conclusions

- Electron spectra simulations in condensed matter systems can be performed: theory and numerics of a method for calculating spectra in systems at any level of aggregation.
- The method is general, the main feature being the calculation of the wf in the continuum.
- I showed application to XPS and Auger spectra to molecules and solids (CO, SiO_2, graphene).
- Advantages of these methods are:
  - Accurate inclusion of correlation effects.
  - Very well scalable with system size (toward biophysics systems).
  - Inclusion of the features of the incident beam

Thanks to:

- Department of Physics, University of Wien and Institute for Solid State Physics, Dresden
  Dr Alex Grüeneis Experimental core level spectroscopy
- Department of Physics, University of Camerino
  Dr Stefano Simonucci Ab-initio calculation of XPS and Auger Electron Spectra
- Department of Physics, University College London
  Prof. D. Alfe' DFT and MD calculations

References

- S.Taioli, S. Simonucci, L. Calliari, M. Filippi, M. Dapor, *Mixed ab initio quantum mechanical and Monte Carlo calculations of secondary emission from Si02 nanoclusters*, Phys. Rev. B 79 (2009) 085432 1-8
- S.Taioli, S. Simonucci, M. Dapor, *SURPRISES: when ab initio meets statistics in extended systems*, Computational Sciences and Discoveries 2 (2009) 015002.
- S.Taioli, S. Simonucci, L. Calliari, M. Dapor, *Electron spectroscopies and inelastic processes in nanoclusters and solids: Theory and experiment* , Physics Reports, accepted and on-line (2010)
- D. Haberer, S. Taioli, S. Simonucci et al., *Tunable band-gap in quasi-free-standing graphene*, accepted for publication in NanoLetters (2010)
- D. Haberer, S. Taioli, S. Simonucci, D. Alfè et al., *Direct observation of a deep acceptor level in electron doped hydrogenated graphene*, submitted to Nature Phys. (2010)

Thank you for your attention!